American Mineralogist
Vol. 57, pp. 1578–1613 (1972)

CORRELATIONS BETWEEN Si–O BOND LENGTH, Si–O–Si ANGLE AND BOND OVERLAP POPULATIONS CALCULATED USING EXTENDED HÜCKEL MOLECULAR ORBITAL THEORY

G. V. Gibbs, M. M. Hamil[1] and S. J. Louisnathan,
Department of Geological Sciences,
Virginia Polytechnic Institute and State University,
Blacksburg, Virginia 24061

and

L. S. Bartell and Hsiukang Yow,
Department of Chemistry,
University of Michigan,
Ann Arbor, Michigan 48104

Abstract

Extended Hückel molecular orbital calculations have been completed for isolated and polymerized tetrahedral ions for ten silicate minerals in which $\Delta\zeta(O) \approx 0.0$ using observed O–Si–O and Si–O–Si valence angles, assuming all Si–O bond lengths are 1.63Å and including silicon 3*s* and 3*p* and oxygen 2*s* and 2*p* atomic orbitals as the basis set. The resultant Mulliken bond overlap populations, n(Si–O), correlate with observed Si–O bond lengths, the shorter bonds being associated with the larger n(Si–O). If the five Si(3*d*) atomic orbitals are also included in the basis set, the observed Si–O(br) and Si–O(nbr) bond lengths correlate with n(Si–O) as two separate trends with overlap populations for the Si–O(nbr) bonds exceeding those for Si–O(br) by about 20 percent, even if the Si–O–Si angle is 180°. Calculation of n(Si–O) as a function of the Si–O–Si angle for the Si–O bonds in $Si_2O_7^{6-}$ (assuming Si–O = 1.63Å and ∢ O–Si–O = 109.47°) first excluding and then including the 3*d*–orbitals, predicts in each case that the Si–O(br) bond lengths should decrease non–linearly and that the Si–O(nbr) bond lengths should increase slightly as the Si–O–Si angle increases.

Scatter diagrams of observed Si–O(br) bond lengths to two–coordinated oxygens versus the Si–O–Si angle appear to vary non–linearly with the shorter bonds tending to occur at wider angles. If these bond lengths are replotted against $-1/\cos(\text{Si–O–Si})$, the scatter diagrams show improved linear trends. Multiple linear and stepwise regression analyses of the bond lengths as a function of $-1/\cos(\text{Si–O–Si})$, $\Delta\zeta(O)$ and $\langle CN \rangle$ indicate that each makes a significant contribution to the variance of the Si–O(br) bond length. The conclusion by Baur (1971) that the Si–O(br) bond length is independent of Si–O–Si angle in silicates for which $\Delta\zeta(O) = 0.0$ can be rejected at the 99 percent confidence level.

Introduction

Pauling (1939) has concluded from the electronegativity difference between Si and O that the Si–O σ–bond has about 50 percent ionic

[1] Now at the Geology Department, Rutgers—The State University, New Brunswick, New Jersey 08903.

character, attributing a charge of about +2 on the silicon atom. Because this charge exceeds +1, thereby violating his electroneutrality principle, he (1952) postulated the formation of d–p π–bonds between the two atoms to neutralize the charge. Using an empirical equation relating interatomic distance to the amount of π–bond character, he then computed a Si–O distance of 1.63Å in close agreement with reported values. Subsequently, Fyfe (1954) calculated semi-empirical bond energies for the SiO_4 tetrahedron as a function of the Si–O separation, and concluded that the relatively short Si–O bond can be explained without resorting to extensive double bonding. On the other hand, Cruickshank (1961) has asserted on the basis of group–theoretic arguments, approximate molecular orbital calculations, and group overlap integrals that of the five $3d$–orbitals, only the two e orbitals on silicon form strong π–bonds with the appropriate $2p\pi$ lone pair orbitals on oxygen. The Si($3d$) orbital involvement in the Si–O bond has since been substantiated by all–electron *ab initio* SCF molecular orbital calculations for the silicate ion and orthosilicic acid (Collins, Cruickshank, and Breeze, 1972). These calculations show (1) that there is considerable Si($3d$)–orbital participation in the wavefunctions with the e orbitals forming π–bonds and the t_2 orbitals forming σ–bonds with the appropriate valence orbitals on oxygen; (2) that the calculated $L_{2,3}$ X–ray fluorescence spectra using $3d$–orbitals are in remarkably good agreement with the experimental spectra of silica glass; the agreement is notably poorer when the $3d$–orbitals are not included in the calculation (see Fig. 1); and (3) that the residual charge on Si is not +4 as assumed in an electrostatic model but is close to zero in reasonable agreement with Pauling's electroneutrality principle and the results of a Si(K)–spectrochemical shift study by Urusov (1967).

Within the last decade a large number of silicate and siloxane structures have been carefully refined using precise diffraction data obtained by modern techniques. These refinements have revealed a number of systematic variations in bond lengths and bond angles: (1) the Si–O(nbr) bonds are usually shorter than the Si–O(br) bonds; (2) shorter Si–O bonds are usually involved in wider O–Si–O and Si–O–Si angles; and (3) the tetrahedral angles usually decrease in the order

$$\measuredangle[\mathrm{O(nbr)–Si–O(nbr)}] > \measuredangle[\mathrm{O(nbr)–Si–O(br)}] > \measuredangle[\mathrm{O(br)–Si–O(br)}].$$

Several investigators have argued that these variations can be rationalized in terms of a covalent model that includes $3d$–orbital involvement between silicon and oxygen (*cf.* Cruickshank, 1961; Lazarev, 1964;

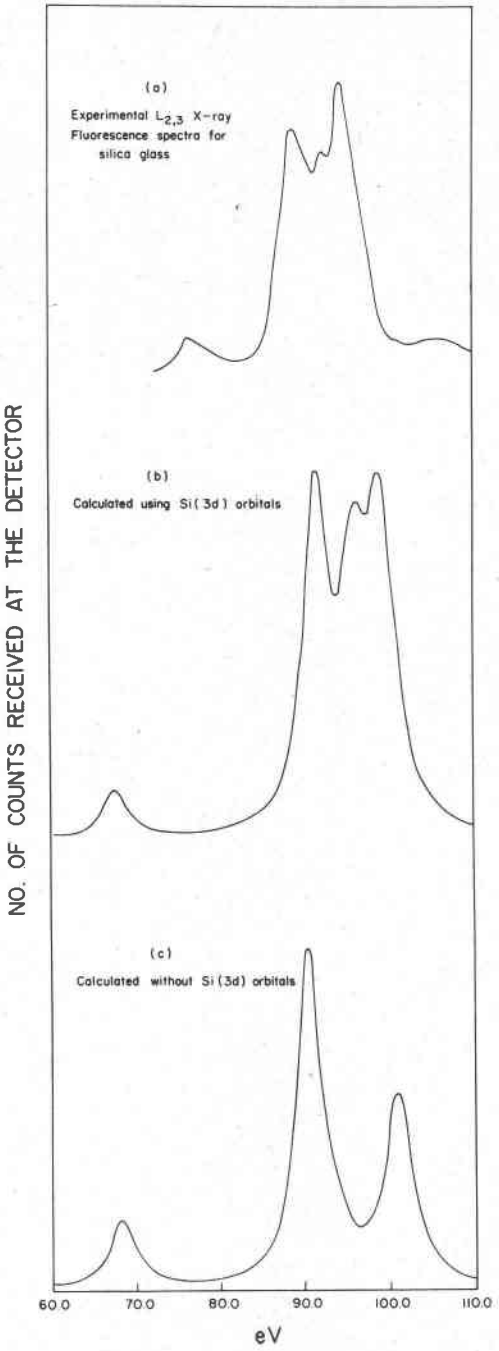

FIG. 1. Comparison of (*a*) the experimental $L_{2,3}$ X-ray fluorescence spectra for silica glass with that calculated by Collins *et al.* (1972) from results obtained in all-electron *ab initio* SFC MO calculations on the silicate ion (*b*) using an extended basis set that includes Si(3*d*) orbitals and (*c*) using a minimum basis set that excludes Si(3*d*) orbitals.

McDonald and Cruickshank, 1967a; Cannillo, Rossi, and Ungaretti, 1968; Bokii and Struchkov, 1968; Noll, 1968; Brown, Gibbs, and Ribbe, 1969; Brown and Gibbs, 1970; Louisnathan and Smith, 1971; Mitchell, Bloss, and Gibbs, 1971). On the other hand, consistency with a covalent model that includes 3*d*–orbital involvement does not, of course, preclude other bonding models. For example, Mitchell (1969) notes that the same trends are implicit both in Gillespie's (1960) valence–shell electron–pair repulsion model and in a molecular orbital model involving a valence basis set of atomic orbitals (without the 3*d*–orbitals of Si).

Despite the systematic variations observed between Si–O bond length and the Si–O–Si and O–Si–O angles in silicates and siloxanes, no attempt has yet been made to rationalize these trends in terms of modern valence theory. An attempt at such a classification should not only serve to improve our understanding and interpretation of such observables as the elastic constants (Wiedner and Simmons, 1972), the bond polarizabilities (Revesz, 1971), the diamagnetic susceptibilities (Verhoogen, 1958), the Raman and infrared spectra (Griffith, 1969) and the X–ray emission and fluorescence spectra (Dodd and Glen, 1969; Urch, 1969; Collins *et al.*, 1972) of silicates in general but should also clarify our understanding of the long–range and short–range forces involved in Al/Si ordering (Stewart and Ribbe, 1969; Brown and Gibbs, 1970).

Recently, Baur (1970, 1971) attempted to rationalize the Si–O bond length variations for a large number of silicates in terms of an electrostatic model by showing that the Si–O bond lengths predicted by his so–called extended electrostatic valence rule correlate well with those observed for structures where $\Delta\zeta(O) \neq 0$[1]. However, he notes that the rule fails to predict bond length variations in silicates like quartz and forsterite where $\Delta\zeta(O) = 0.0$. In spite of this shortcoming, Baur has rejected Cruickshank's double bonding model in favor of an electrostatic

[1] For Si–O bond length variations in the tetrahedral portion of a silicate, the extended electrostatic valence rule states that the deviation of an individual Si–O bond from the mean length, $\langle$Si–O$\rangle$, in a silicate ion is proportional to $\Delta\zeta(O)$. The actual bond length is predicted by the empirical equation

$$\text{Si–O}_{\text{pred.}} = \langle\text{Si–O}\rangle + 0.091\ \Delta\zeta(O)$$

where $\Delta\zeta(O) = \zeta(O) - \bar{\zeta}(O)$, $\zeta(O)$ is the sum of the Pauling (1929; 1960) bond strengths received by oxygen and $\bar{\zeta}(O)$ is the mean $\zeta(O)$ for the silicate ion under consideration. Baur (1970, 1971) uses p_O instead of $\zeta(O)$ to denote the sum of the bond strengths received by oxygen. However, we prefer to retain Pauling's symbolism for two reasons: (1) $\zeta(O)$ is an accepted symbol used by many investigators and (2) p denotes bond–order or bond–number in modern valence theory (*cf.* Coulson, 1939; Pople *et al.*, 1965; and Mulliken, 1955).

model (1) because he could not *prove* a dependence between Si–O bond length variation and Si–O–Si angle for five silica polymorphs[1] and four disilicates where $\Delta\zeta(O) = 0.0$ and (2) because the Si–O bond length variations in 26 structures containing disilicate ions (where $\Delta\zeta(O) \neq 0$ for the most part) show a better correlation when plotted against $\Delta\zeta(O)$ than when plotted against $\measuredangle$ [Si–O–Si]. Even though the latter result suggests that more of the variation in bond length may be explained in terms of $\Delta\zeta(O)$ than in terms of the angle, it cannot be concluded *a priori* that the bond length variation is independent of the angle without appropriate statistical tests.

According to Baur (1971), the main difference between his electrostatic model and Cruickshank's double bonding model is that the latter stresses the importance of the intrinsic electronic structure of the tetrahedral ions whereas his electrostatic model stresses the extrinsic effects from the the non–tetrahedral cations. Although Baur is aware of the empirical nature of his model and the fact that it certainly cannot replace a model based on electronic structure, he has stated that future models for the Si–O bond (1) should incorporate the electronic structure of the constituent atoms as well as the effects of the non–tetrahedral cations and (2) should begin where his electrostatic model breaks down (for minerals like forsterite, quartz, *etc.*). The Si–O bond length variations in forsterite were recently examined in terms of extended Hückel molecular orbital (EHMO) theory by Louisnathan and Gibbs (1971) who found that the observed bond length variations show a close correspondence with bond overlap populations, n(Si–O), calculated (1) for the silicate ion alone and (2) for the silicate ion with its nearest neighbor non–tetrahedral cations and their ligands.

[1] The relationship between Si–O distance and Si–O–Si angle for the silica polymorphs was recently re–examined by D. Taylor (1972); see *Mineral. Mag.* **38**, 629–631. After correcting the Si–O distances in the polymorphs for thermal motion of the oxygen atoms, Taylor calculated a regression line for the corrected Si–O bond lengths and their associated Si–O–Si angles. He found the resulting line to be less steep than those calculated earlier by Brown *et al.* (1969) for the framework silicates but statistically identical to the one calculated in our study (see Table 3). Moreover, Taylor notes the probability the slope of the line might be zero is a little less than 0.05, a result at variance with the findings by Baur (1971) who believes that a dependence between Si–O distance and Si–O–Si angles does not exist for minerals like the silica polymorphs where $\Delta\zeta(O) = 0.0$.

n(Si–O) calculated with Si(*spd*) valence basis set for the silicate ion in forsterite

Bond Length	(1) For the silicate ion alone n(Si–O)	(2) With non–tetrahedral cations and their ligands n(Si–O)
Si–O(1) = 1.613Å	0.935	1.003
Si–O(2) = 1.654	0.878	0.931
Si–O(3) = 1.635	0.892	0.968

The n(Si–O) calculated for the silicate ion alone (see col. 1 above) were made using the observed O–Si–O angles but with all Si–O distances set equal to 1.63Å. Despite the assumption in the calculation that all Si–O bond lengths are constant, it is clear that the resulting n(Si–O) can be used to order the observed Si–O bond lengths in forsterite. Encouraged by this result, the present study was undertaken to learn whether or not EHMO theory can serve as a model for classifying and ordering Si–O bond length variations when the non–tetrahedral cations are ignored and $\Delta\zeta(O) \approx 0.0$. Moreover, in the event that these calculations prove successful, they should improve our understanding of the nature of the Si–O bond in terms of modern valence theory and provide plausible reasons for the variation of individual Si–O bond lengths in silicates and siloxanes in general. In addition, new scatter diagrams of Si–O(br) bond length plotted against Si–O–Si angle will be presented for data from 31 carefully refined silicate and several siloxane structures in which $\Delta\zeta(O)$ is zero or small. The relative contributions of Si–O–Si, $-1/\cos$(Si–O–Si), $\Delta\zeta(O)$, and $\langle CN \rangle$ (the mean coordination number of oxygen bonded to silicon) to the Si–O(br) bond length in these structures will be assessed using multiple linear and stepwise regression methods[1] (see appendix). The outcome of the analysis will show that we can reject the hypothesis that a relationship between Si–O(br) and Si–O–Si angle might not exist for silicates where $\Delta\zeta(O) = 0.0$.

The Calculation and Significance of Bond Overlap Populations Obtained in the Extended Hückel Molecular Orbital Theory

Since Pauling (1929) formulated his famous set of rules for predicting stable atom configurations in ionic crystals, many silicate structures have been investigated by X–ray methods and have been found

[1] Linear, multiple linear, and stepwise linear regression computations presented in our paper were completed using the UCLA BIOMEDICAL PROGRAM PACKAGE, 1967.

to conform remarkably well. Nevertheless, the steric details of the tetrahedral ions in many of these same silicates also appear to conform with a model that includes covalent bonding (*cf.* Brown *et al.*, 1969; Brown and Gibbs, 1970). In an attempt to learn whether these details are indeed consistent with covalent theory, extended Hückel molecular orbital calculations were made for the tetrahedral ions in ten silicate minerals specifically chosen such that $\Delta\zeta(O)$ is either zero or small. In this way the importance of the intrinsic electronic structure of the tetrahedral ions can be emphasized to the reader (Hamil, Gibbs, Bartell and Yow, 1971). Silicates showing a larger variation in $\Delta\zeta(O)$ will be considered elsewhere by Louisnathan and Gibbs in a study of the disilicates (1972d). EHMO calculations, although very inexpensive and crude by *ab initio* standards (Richards and Horsley, 1970), have been moderately successful in generating Walsh–Mulliken diagrams (molecular orbital energies plotted against bond angle) (*cf.* Hoffmann, 1963; Gavin, 1969; Allen, 1970; 1972) and in delineating trends in variations of bond length with bond overlap populations or bond order for a number of relatively large molecules in their ground states (*cf.* Dallinga and Ross, 1968; Gavin, 1969; Boyd and Lipscomb, 1969). Recently, Bartell, Su, and Yow (1970) calculated EHMO bond overlap populations for the tetrahedral bonds in selected sulfates and phosphates and found that they show strong correlations with (1) the simple valence bond orders assigned by Cruickshank (1961) and (2) the observed tetrahedral bond lengths. To learn whether Si–O bond overlap populations for the silicates show similar trends, calculations were undertaken using an EHMO program originally written by Hoffmann (1963). In the calculations, one-electron molecular orbitals, MOs, are constructed as a linear combination of atomic orbitals, LCAO,

$$\Psi_k = \sum_{i=1}^{n} c_{ki}\phi_i$$

where c_{kj} are the linear coefficients and ϕ_j the Slater type single exponent atomic valence orbitals. The energy associated with an MO, ϵ_k, is obtained by diagonalizing the secular determinant $|H_{ij} - \epsilon S_{ij}| = 0$, where S_{ij} are the two center overlap integrals (explicitly evaluated from the positional coordinates of the constituent atoms), and H_{ij} are the elements of the Hückel Hamiltonian matrix. In the rigorous Roothaan–Hartree–Fock method, the H_{ij} are complicated functions of the linear coefficients and of two–, three–, and four–centered integrals, and this fact requires an iterative solution of the secular equation (Richards and Horsley, 1970). On the other hand, in EHMO theory

the H_{ii} terms are not explicitly evaluated but are chosen to simulate spectroscopically obtained quantities, namely the negative of the valence orbital ionization potentials (VOIP) whereas the H_{ij} terms are approximated by the Wolfsberg–Helmholz (1952) parametrization

$$H_{ij} = S_{ij}(H_{ii} + H_{jj}).$$

When one–electron MOs are constructed and their energies obtained, the Pauli exclusion principle is applied as an afterthought and the MOs are filled with electrons pair–wise starting from the lowest eigenstate. By inserting eigenvalues, ϵ_k, into the set of secular equations,

$$\sum_{i=1}^{n} (H_{ij} - \epsilon_k S_{ij})c_{kj} = 0,$$

the linear coefficients c_{kj} are evaluated but they are not in any way refined to self–consistency. It is important to note that trends in these linear coefficients depend in large part on the geometry of the tetrahedral ions modeled in our calculations. Finally, a Mulliken (1955) population analysis is completed to obtain the desired Si–O bond overlap populations,

$$n(\text{Si–O}) = 2 \sum_{k}^{\text{MO}} N(k) \sum_{i \varepsilon \text{Si}} \sum_{j \varepsilon \text{O}} c_{ki}c_{kj}S_{ij},$$

using the overlap integrals, the linear coefficients and the number of electrons, $N(k)$, (0, 1, or 2) in MO Ψ_k. The bond overlap populations provide numerical estimates of the strength of covalent bonding and anti–bonding between two atoms. Two atoms are considered to be bonded when the overlap population is positive, nonbonded when it is zero, and antibonded when it is negative; short bonds are usually involved with large overlap populations and longer bonds with smaller ones. If observed Si–O bond lengths are used in the calculation of n(Si–O), the shorter bonds, which usually have larger overlap integrals, S_{ij}, will tend to have larger bond overlap populations than longer bonds. As it is important to be able to discriminate between this induced correlation and that induced by the geometrical aspects of the tetrahedral ions, we have undertaken two separate calculations (1) using the observed O–Si–O and Si–O–Si angles and clamping all Si–O distances at 1.63Å and (2) using the observed distances and angles. By clamping all the Si–O at 1.63Å, the correlation between n(Si–O) and the observed Si–O bond length induced by the overlap integrals is effectively removed and what remains should be related to the intrinsic electronic structure of the ions induced in large part by such

geometrical factors as the O–Si–O and Si–O–Si angles. Because of the very crude nature of the EHMO method intrinsic in the very daring approximations outlined above and because of the utter neglect of the screening potential produced by the Coulomb and exchange interactions, little significance can be attached to the *actual numbers* obtained for n(Si–O). However, it is the trends between the calculated n(Si–O) and the experimentally determined Si–O bond lengths that are considered significant, *not* the absolute numbers for any one tetrahedral ion. Thus, EHMO results can be useful in *ordering* and *classifying* observed bond lengths with bond overlap populations but it *cannot* be used to *prove* the observed bond length variations nor can it be used to *prove* the participation of the 3*d*–orbitals of Si in the wave functions calculated for the ions studied.

The VOIP and orbital exponents used as input to the program are given in Table 1. For the *s*– and *p*– orbitals the free–atom optimized orbital exponents of Clementi and Raimondi (1963) were chosen together with VOIP similar to the zero–charge values of Basch, Viste, and Gray (1965). For the 3*d* orbitals of silicon, an orbital exponent significantly higher than the Slater–rule value was adopted for reasons discussed by Bartell *et al.* (1970), and $H_{3d,3d}$ was adjusted to −5.5 eV to yield orbital and overlap populations comparable, in the case of SiH_4, to *ab initio* populations found by Boer and Lipscomb (1969). These parameters gave 3*d* populations in SiO_4^{4-} which turned out to be of the same magnitude as the *ab initio* populations reported subsequently by Collins *et al.* (1972).

A fundamental weakness of the extended Hückel scheme (which is not based on a *bona fide* Hamiltonian) is that its energies and wave functions are sensitive to the somewhat arbitrary parameterization adopted and, accordingly, have only a qualitative significance. On the other hand, the EHMO *trends* in charge distributions and bond popu-

TABLE 1. VALENCE ORBITAL IONIZATION POTENTIALS (VOIP) AND ORBITAL EXPONENTS (ξ).

Atom	Atomic Orbital	VOIP (eV)	ξ
Oxygen	2*s*	−32.33	2.246
	2*p*	−15.79	2.227
Silicon	3*s*	−14.19	1.634
	3*p*	−8.15	1.428

lations in a series of related molecules have been found to be insensitive to the exact parameterization; they are also roughly independent of whether the VOIP are frozen at plausible values or are adjusted to self-consistency with atomic charges (Basch *et al.*, 1965). Therefore, since the present investigation is a preliminary exploration of *trends* in a series of structures, it seemed adequate to choose the simplest variant of the extended Hückel method with fixed VOIP and exponents. Finally, it is important to note that one of the biggest deficiencies of the extended Hückel method is its failure to take adequate account of the Coulomb interactions. The method works the best for molecules where the electronegativity difference, $\Delta\chi$, between bonded atoms is small. However, it starts to break down when $\Delta\chi$ is greater than approximately 1.3, the breakdown being complete when $\Delta\chi \geq 2.5$ (Allen, 1970). Thus, when heteropolar substances with intermediate bond type (like the Si–O bond in a silicate where $\Delta\chi = 1.7$) are studied, EHMO theory may be used to qualitatively diagnose the covalent aspects of the bonding. Accordingly, it is of particular interest to apply the EHMO method to silicate structures which have been found to conform remarkably well in the past with Pauling's rules[1] for ionic crystals yet which also conform in many instances with a model that includes covalent bonding.

The Relationship Between Si–O(br) Bond Overlap Population and the O–Si–O and Si–O–Si Angles

In a study of several orthosilicates, Louisnathan and Gibbs (1972a) have found that the tetrahedral valence angles in hypothetically distorted SiO_4 tetrahedra have a pronounced effect on n(Si–O), the wider O–Si–O angles being associated with bonds of larger overlap populations. They also showed for a number of silicates (1972b) that a correlation can be made between the mean of three O–Si–O angles, $\langle$O–Si–O$\rangle_3$, and the length of the Si–O bond common to these three angles, shorter bonds tending to be associated with larger values of $\langle$O–Si–O$\rangle_3$. McDonald and Cruickshank (1967a) and more recently Brown and Gibbs (1970) have also shown that shorter Si–O distances are typically involved in wider O–Si–O angles. Although Baur (1970) has also indicated that shorter Si–O distances tend to be involved in wider O–Si–O angles, his geometrical model of a Si atom rattling

[1] According to Bent (1968) Pauling's rules may have a more universal application as structural principles than heretofore realized because when suitably rationalized they may apply to covalent as well as ionic compounds, perhaps even to metallic compounds.

within a *rigid* tetrahedron of oxygen spheres is not realized in general in the silicates (Louisnathan and Gibbs, 1972b).

The Si–O–Si angles in silicates (Liebau, 1961) and in siloxanes (Noll, 1956) are usually between 130° and 140°, although angles as wide as 180° are not uncommon. Except for an angle of 93° in Si_2O_2 (Anderson and Ogden, 1969), angles less than 120° are rare. A bonding model that includes Si(3*d*) orbital participation predicts that the length of the Si–O(br) bond should increase as the Si–O–Si angle becomes narrower (Cruickshank, 1961). Moreover, as the Si–O–Si angle narrows, increasing electrostatic repulsions between the Si–atoms and decreasing *s*–character in the O(br)–orbitals (*i.e.*, a decreasing σ–bond strength) are additional factors that are predicted to lengthen Si–O(br) (Cruickshank, 1961; Brown *et al.*, 1969).

In a re–investigation of the crystal structure of zunyite, Louisnathan and Gibbs (1972c) have found that the size of the tetrahedral angles has a pronounced effect on n[Si–O(br)] in $Si_2O_7^{6-}$ ions with linear Si–O–Si linkages. Thus, if $\sphericalangle$[O(br)–Si–O(nbr)] > $\sphericalangle$[O(nbr)–Si–O(nbr)], then n[Si–O(br)] > n[Si–O(nbr)]. However, if $\sphericalangle$[O(br)–Si–O(nbr)] $\approx$ $\sphericalangle$[O(nbr)–Si–O(nbr)], then n[Si–O(br)] $\approx$ n[Si–O(nbr)] whereas if $\sphericalangle$[O(br)–Si–O(nbr)] < $\sphericalangle$[O(nbr)–Si–O(nbr)] then n[Si–O(br)] < n[Si–O(nbr)] (see Fig. 2). These results calculated with all Si–O bond lengths clamped at 1.63Å imply that the magnitude of the tetrahedral angles plays an important role in establishing n[Si–O(br)] in the Si–O(br)–Si linkage. In order to assess the nature of the relationship between the Si–O(br) bond length and Si–O–Si angle, we calculated n[Si–O(br)] as a function of Si–O–Si angle for the three $Si_2O_7^{6-}$ ions shown in Figure 2. The results calculated with Si–O = 1.63Å and a Si(*sp*) valence basis set are presented in Figure 3a. Regardless of the size of the tetrahedral angles, n[Si–O(br)] increases *non–linearly* with increasing Si–O–Si angle, the largest overlap population being associated with the 180° angle. Analyses of the linear coefficient, c_{ki}, and the overlap, S_{ij}, matrices indicate that the change in n[Si–O(br)] is related to concomitant changes in both the σ– and π–bonding potentials. In other words, widening of the Si–O–Si angle increases both the σ– and π–bond strengths as proposed by Cruickshank (1961), Brown *et al.* (1969), and Brown and Gibbs (1970). Using results provided by the theory of atomic orbital hybridization, Louisnathan and Gibbs (1972c) have proposed that the Si–O(br) bond length should vary as a function of $-1/\cos$ (Si–O–Si). When the n[Si–O(br)] are replotted as a function of $-1/\cos$ (Si–O–Si), a well–defined linear relation (Fig. 4) is realized.

The trends predicted by EHMO theory are similar whether or not the Si(3*d*) orbitals are included in the calculation (Figs. 3a and 3b),

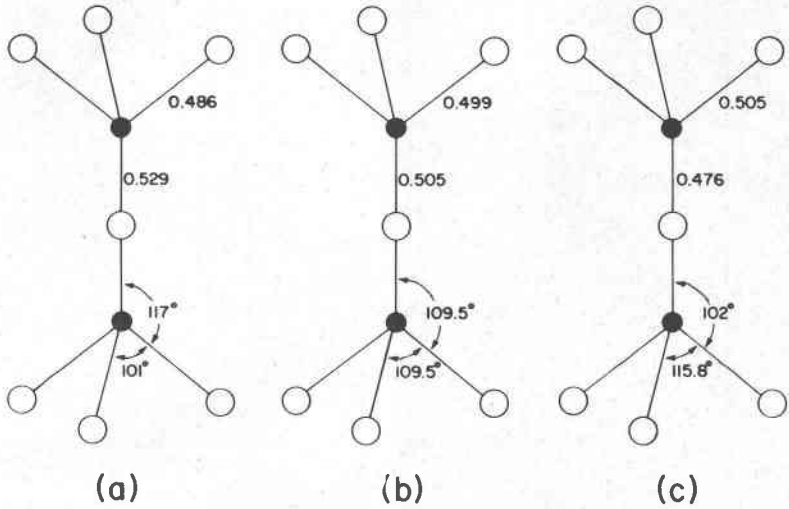

FIG. 2. A comparison of Si-O bond overlap populations (the decimal fractions listed adjacent to the Si–O(br) and Si–O(nbr) bonds) calculated for three $Si_2O_7^{6-}$ ions (D_{3h} point symmetry with C_3 along the Si–O–Si linkage) where (*a*) ∢[O(br)–Si–O (nbr)] > ∢[O(nbr)–Si–O(nbr)], (*b*) ∢[O(br)–Si–O(nbr)] = ∢[O(nbr)–Si–O(nbr)] and (*c*) ∢[O(br)–Si–O(nbr)] < ∢[O(nbr)–Si–O(nbr)]. The calculation was made using a Si(*sp*) valence basis and with all Si–O = 1.63Å. Note that *n*[Si–O(br)] > *n*[Si–O(nbr)] for the conformation in (*a*), *n*[Si–O(br)] ≃ *n*[Si–O(nbr)] for (*b*) and that *n*[Si–O(br)] < *n*[Si–O(nbr)] in (*c*). (See Louisnathan and Gibbs, 1972c).

suggesting that the observed steric details of a tetrahedral ion in a silicate may not be used to establish the involvement of the 3*d*–orbitals in the formation of the Si–O bond. This is in agreement with Mitchell's (1969) assertion that "one cannot . . . expect experiments to establish whether *d*–orbitals are 'really' used anymore than experiments can show *s* and *p* orbitals definitely occur in bonding of the first row elements" (see also Bartell *et al.*, 1970).

Si–O Bond Length Variation in Low–Quartz, Low–cristobalite, and Coesite

The silica polymorphs are possibly the most appropriate structures for examining the dependence of Si–O(br) bond length on both the O–Si–O and Si–O–Si angles, because (1) there are no bonds other than Si–O(br), (2) all oxygens are two–coordinated and bridge two tetrahedra, and (3) $\Delta\zeta(O) = 0$. For our analysis, we have chosen data from three precisely refined structures, all with e.s.d.'s less or equal to 0.006Å: low–quartz (Zachariasen and Plettinger, 1965), low–cristobalite (Dollase, 1965), and coesite (Araki and Zoltai, 1969) (Group A

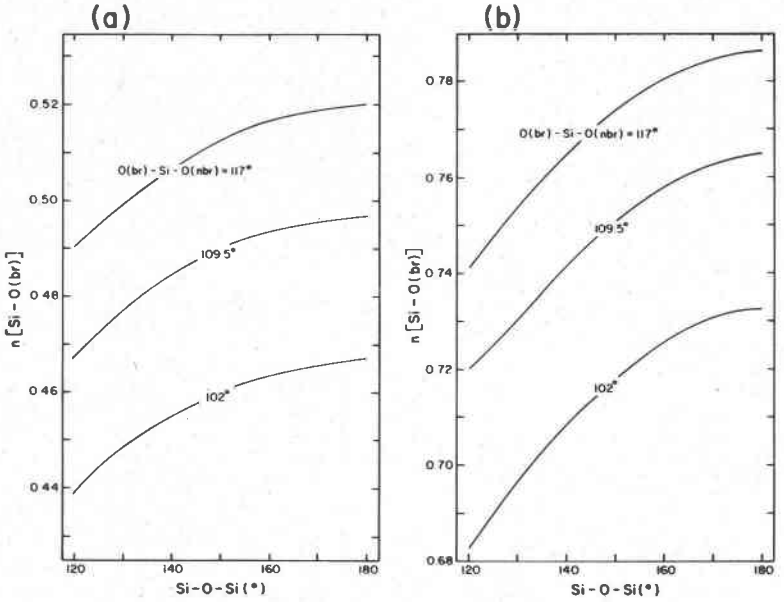

FIG. 3. Si–O(br) bond overlap populations calculated as a function of the Si–O–Si angle for the three pyrosilicate ions depicted in Figure 2. (*a*) Si(*sp*) basis with all Si–O = 1.63Å and (*b*) Si(*spd*) basis with all Si–O = 1.63Å. Si–O(nbr) bond overlap populations for each ion increase only slightly with Si–O–Si and accordingly are not shown.

in Table 2). The data for keatite and low–tridymite were not included in the analysis for reasons given in the next section. The three structures chosen provide twelve individual Si–O(br) bond lengths varying from 1.598 to 1.631Å. Figure 5c is a scatter diagram of Si–O(br) bond length versus $\langle$O–Si–O$\rangle_3$ angle; Figure 5*b* shows Si–O(br) versus [$-1/\cos$(Si–O–Si)]. Using the estimated standard error of the slopes for the lines fitted to the distributions in Figures 5*c* and 5*b* (see Table 3), the null hypothesis can be tested that the true slope in each case is zero; that is, that the Si–O(br) bond length is independent of $\langle$O–Si–O$\rangle_3$ or $-1/\cos$(Si–O–Si). Student's $|t|$ calculates to be 3.3 and 2.3 for the data in Figures 5*c* and 5*b* respectively (Table 3). Since these values exceed the 90 percent confidence level (*cf.* Draper and Smith, 1966) of $t(10, 0.90) = 1.4$, we can reject the hypothesis that a relationship between Si–O(br) and $-1/\cos$(Si–O–Si) or $\langle$O–Si–O$\rangle_3$ might not exist.

We have used the function [$-1/\cos$(Si–O–Si)] rather than the angle itself because n[Si–O(br)] vary non–linearly with the angle but

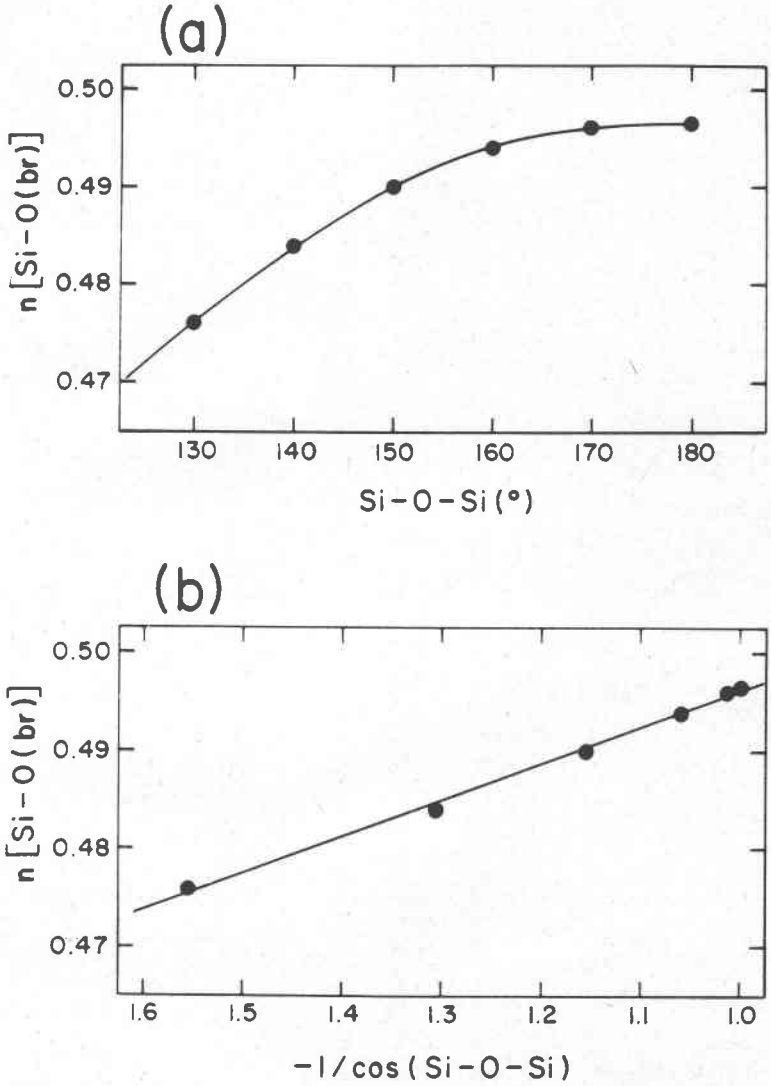

FIG. 4. Plots of n[Si–O(br)] as a function of (*a*) Si–O–Si angle and (*b*) —1/cos(Si–O–Si) where the bond overlap population was calculated for the conformation in Figure 2b and a Si(*sp*) basis set.

linearly with $[-1/\cos(\text{Si–O–Si})]$ (Fig. 4). However, even if the relationship between Si–O(br) bond length and Si–O–Si angle is assumed to be linear, the hypothesis of no interdependence can again be rejected at the 90 percent confidence level (see Table 3). When the Si–O(br) lengths are estimated using the intercept and coefficients obtained from a multiple linear regression analysis, using both $\langle\text{O–Si–O}\rangle_3$ and $[-1/\cos(\text{Si–O–Si})]$ as independent variables, a reasonable correspondence between the experimental and estimated distances is observed (Fig. 5*c* and Table 2). Finally, two comments on Figures 5*a* and 5*b* are worth making: (1) the quantity $[-1/\cos(\text{Si–O–Si})]$ may be a better defined variable than $\langle\text{O–Si–O}\rangle_3$ because the former includes a more accurate account of the hybridization characteristics on O(br) than the latter does of the hybridization characteristics of Si, and (2) the calculated slope $[-0.05(2)]$ for Figure 5*b* is statistically identical with that $[-0.034(1)]$ obtained for $n[\text{Si–O(br)}]$ versus $[-1/\cos(\text{Si–O–Si})]$ (Fig. 4b), an interesting coincidence de-

Table 2

Si–O(br) bond lengths, Si–O(br)–Si angles, oxygen mean coordination number, <CN>, and $\Delta\zeta(O)$ for silica polymorphs, silicates and siloxanes

Group A: Si–O(br) bond distance vs. Si–O(br)–Si angle data for silica polymorphs where $\Delta\zeta(O)=0.0$ and <CN>=2.0

		Si–O(br)	<Si–O(br)>	Si–O–Si	$\frac{-1}{\cos(\text{Si–O–Si})}$	<CN>	$\Delta\zeta(O)$	Reference
Low Cristobalite	Si–O(1) Si–O(2)	1.601 1.608	1.6045	146.8	1.1951	2.0	0.0	Dollase (1965)
Coesite	Si(1)–O(1) Si(2)–O(2)	1.600 1.608	1.600 1.608	180.0 143.8	1.0000 1.2392	2.0 2.0	0.0 0.0	Araki and Zoltai (1969)
	Si(1)–O(3) Si(2)–O(3)	1.607 1.619	1.613	145.0	1.2208	2.0	0.0	
	Si(1)–O(4) Si(2)–O(4)	1.598 1.625	1.6115	150.4	1.1501	2.0	0.0	
	Si(1)–O(5) Si(2)–O(5)	1.631 1.617	1.6240	136.1	1.3878	2.0	0.0	
Quartz	Si–O(1) Si–O(1)'	1.603 1.616	1.6095	143.5	1.2440	2.0	0.0	Zachariasen & Plettinger (1965)

Group B: Si–O(br) bond distance vs. Si–O(br)–Si angle data for silicates and siloxanes where $\Delta\zeta(O)=0.0$ for all oxygens

Hemimorphite	Si–O(4)	1.627	1.627	150.3	1.1512	2.8	0.0	McDonald & Cruickshank(1967b)
Benitoite	Si–O(1) Si–O(1)'	1.630 1.648	1.639	132.9	1.4690	2.7	0.0	Fischer (1969)
Thortveitite	Si–O(1)	1.6052	1.6052	180.0	1.0	2.9	0.0	Prewitt (personal comm.)
Beryl	Si–O1(2) Si–O1(1)	1.594 1.595	1.5945	168.8	1.0194	2.7	0.0	Gibbs, Breck and Meagher (1968)
Emerald	Si–O1(2) Si–O1(1)	1.604 1.585	1.5945	169.3	1.0177	2.7	0.0	
$H_3Si\text{–}O\text{–}SiH_3$		1.634	1.634	144.1	1.2345	2.0	0.0	Almenningen et.al., (1963)
$(CH_3)_6(SiO)_3$		1.635	1.635	131.6	1.5062	2.0	0.0	Oberhammer (1972)
$(CH_3)_8(SiO)_4$		1.622	1.622	144.8	1.2238	2.0	0.0	
$(CH_3)_{10}(SiO)_5$		1.620	1.620	146.2	1.2034	2.0	0.0	
$(CH_3)_{12}(SiO)_6$		1.622	1.622	149.6	1.1594	2.0	0.0	
$Yb_2Si_2O_7$	Si–O(1)	1.626	1.626	180.0	1.0	2.9	0.0	Smolin & Shepelev (1970)
$Er_2Si_2O_7$	Si–O(1)	1.632	1.632	180.0	1.0	2.9	0.0	

Table 2 (cont.)
Group C: Si-O(br) bond distance vs. Si-O(br)-Si angle data for silicates where O(br) is two coordinated

$Ba_3Si_4Nb_6O_{26}$	Si-O(1)	1.599	1.599	180.0	1.0000	3.7	-.10	Shannon and Katz (1970)
Low Albite	$Si_1(m)-O_B(m)$	1.603	1.610	161.2	1.0564	2.9	-.04	Ribbe et.al., (1969)
	$Si_2(O)-O_C(m)$	1.617					.02	
	$Si_1(m)-O_C(m)$	1.622	1.6185	135.7	1.3972	2.9	-.04	
	$Si_1(m)-O_D(m)$	1.615					-.04	
Low Cordierite	Si(3)-O(6)	1.603	1.6115	176.5	1.0019	2.7	.02	Gibbs (1966)
	Si(4)-O(6)	1.620					.02	
Haddam Cordierite	Si(3)-O(6)	1.601	1.6055	179.6	1.0000	2.7	.02	Meagher (1967)
	Si(4)-O(6)	1.610					.02	
Danburite	Si-O(1)	1.614	1.614	136.8	1.3718	3.7	-.26	Phillips et.al., (1971)
Krauskopfite	Si(1)-O(4)	1.634	1.644	131.9	1.4974	3.4	-.09	Coda et.al., (1967)
	Si(2)-O(4)	1.654					.05	
Maximum Microcline	$Si_1(m)-O_C(m)$	1.629	1.631	130.8	1.5304	2.9	-.04	Brown and Bailey (1964)
	$Si_2(O)-O_C(m)$	1.633					-.04	
	$Si_2(m)-O_B(m)$	1.617	1.6125	155.9	1.0955	2.9	.02	
	$Si_1(m)-O_B(m)$	1.608					-.04	
Kinoite	Si(1)-O(2)	1.626	1.634	140.1	1.3035	2.4	.05	Laughon (1971)
	Si(2)-O(2)	1.642					-.03	
Epididymite	Si(1)-O(4)	1.605	1.6175	151.5	1.1379	2.8	-.02	Robinson and Fang (1970)
	Si(2)-O(4)	1.630					-.04	
	Si(1)-O(1)	1.606	1.606	143.8	1.2392		.00	
	Si(2)-O(6)	1.629	1.629	143.0	1.2521		.07	
	Si(3)-O(8)	1.633	1.633	139.0	1.3250		.01	
Actinolite	Si(1)-O(7)	1.621	1.621	141.1	1.2850	3.2	-.13	Mitchell et.al., (1971)
Cummingtonite	Si(1)-O(7)	1.613	1.613	142.2	1.2622	3.0	-.03	
	Si(1)-O(5)	1.614	1.6265	139.7	1.3112		-.03	
	Si(2)-O(5)	1.639					.00	
Grunerite	Si(1)-O(7)	1.613	1.613	144.8	1.2238	3.0	-.03	Finger (1969)
	Si(1)-O(5)	1.627	1.619	142.4	1.2622		-.03	
	Si(2)-O(5)	1.611					.00	
Tremolite	Si(1)-O(7)	1.616	1.616	139.3	1.3190	3.2	-.13	Papike et.al., (1969)
Glaucophane	Si(1)-O(7)	1.611	1.611	147.2	1.1897	3.2	-.11	
C-centered Mn-Cummingtonite	Si(1)-O(7)	1.616	1.616	141.0	1.2868	3.0	-.03	
	Si(1)-O(5)	1.622	1.628	140.0	1.3054		-.03	
	Si(2)-O(5)	1.634					.00	
Primitive Mn-Cummingtonite	Si(1)-OA(7)	1.628	1.628	139.1	1.3230	3.0	-.03	
	Si(1)-OA(5)	1.607	1.622	139.8	1.3092		-.03	
	Si(2)-OA(5)	1.637					.00	
	Si(1)-OB(7)	1.603	1.603	141.0	1.2868		-.03	
	Si(1)-OB(5)	1.634	1.6345	138.4	1.3373		-.03	
	Si(2)-OB(5)	1.635					.00	
Protoamphibole	Si(1)-O(7)	1.624	1.624	137.1	1.3651	3.1	-.07	Gibbs (1969)
	Si(1)-O(5)	1.616	1.621	140.6	1.2941		-.07	
	Si(2)-O(5)	1.626					.03	
Anthophyllite	Si(1)-OA(7)	1.615	1.615	141.4	1.2796	3.2	-.07	Finger (1970)
	Si(1)-OA(6)	1.611	1.616	140.8	1.2904		-.07	
	Si(2)-OA(6)	1.621					.03	
	Si(1)-OB(7)	1.617	1.617	137.8	1.3499		-.14	
Clinozoisite	Si(1)-O(9)	1.628	1.6275	164.3	1.0387	3.5	-.03	Dollase (1968)
	Si(2)-O(9)	1.627					.11	
Piedmontite	Si(1)-O(9)	1.638	1.636	151.0	1.1434	3.5	-.03	Dollase (1969)
	Si(2)-O(9)	1.634					.11	
Epidote	Si(1)-O(9)	1.640	1.634	153.6	1.1164	3.5	-.03	Dollase (1971)
	Si(2)-O(9)	1.628					.11	

spite the fact that all n(Si–O) were calculated assuming all Si–O equal 1.63Å and all O–Si–O angles = 109.47° in Figure 4.

The Correlation Between Si–O(br) Bond Length and Si–O–Si Angle in Structures Where $\Delta\zeta$(O) is Zero

In structures of low–quartz, low–cristobalite, coesite, hemimorphite, thortveitite, beryl, emerald, benitoite, $Yb_2Si_2O_7$, $Er_2Si_2O_7$, and five siloxanes, all the oxygen atoms receive the same bond strength, *i.e.*

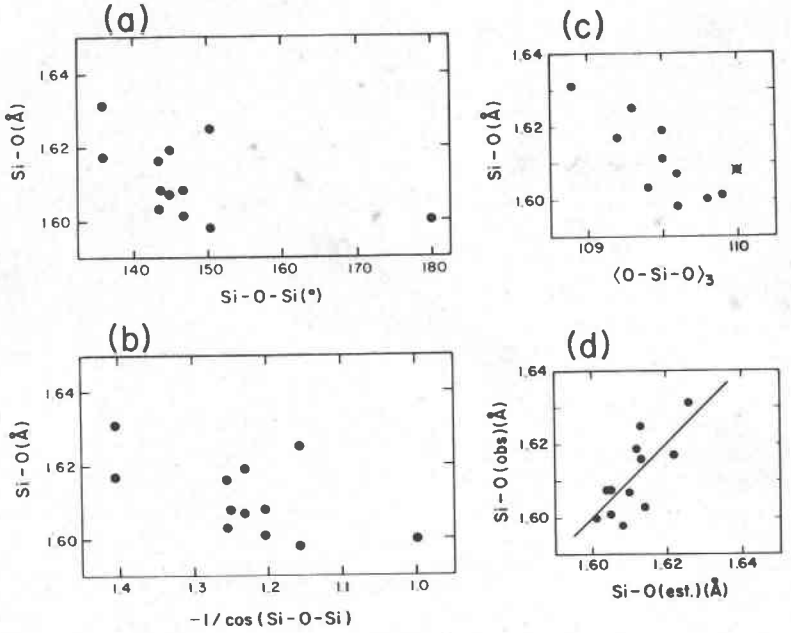

FIG. 5. Scatter diagrams of Si–O(br) bond length data from Table 2, group A, plotted as a function of (*a*) Si–O–Si, (*b*) $-1/\cos$(Si–O–Si), (*c*) $\langle$O–Si–O$\rangle_3$ = the average of the three O–Si–O angles involving a common Si–O bond and (*d*) Si–O(est.)Å using the results of a multiple linear regression analysis with $-1/\cos$(Si–O–Si) and $\langle$O–Si–O$\rangle_3$ as independent variables.

$\zeta(O) = 2.0$ and $\Delta\zeta(O) = 0.0$. The Si–O(br) bond lengths and Si–O–Si angles in these structures are listed in Table 2 (Groups A and B). The scatter diagram of Si–O(br) versus Si–O–Si angle and [$-1/\cos$(Si–O–Si)] are given in Figures 6*a* and 6*b*, respectively. For the 27 individual Si–O(br) bond lengths in this data set, the hypothesis that the true slopes of (1) Si–O(br) versus Si–O–Si angle and of (2) Si–O(br) versus [$-1/\cos$(Si–O–Si)] are zero was tested. The calculated intercepts, slopes, partial correlation coefficients, and $|t|-$ values are given in Table 3. The calculated $|t|-$ values are 2.5 and 3.6 for Figures 6*a* and 6*b*, respectively. Because these $|t|$s exceed the critical value of $t(25, 0.90) = 1.3$, we can reject the null hypothesis that Si–O(br) bond length and Si–O–Si angle might not be correlated (actually 2.5 also exceeds $t(25, 0.99)$). This result is contrary to Baur's (1971) conclusion that a correlation cannot be made between Si–O(br) and Si–O–Si angle for silicates where $\Delta\zeta(O) = 0$. He reached his conclusion using data from keatite, high–tridymite, low–quartz, low–

cristobalite, coesite, $Yb_2Si_2O_7$, $Er_2Si_2O_7$, hemimorphite, and thortveitite. We have omitted the data for keatite in our analysis because as Baur (1970) has indicated they are "demonstrably poor." The data for high–tridymite were also omitted because of the large e.s.d.'s in its atomic coordinates and because the Si–O–Si angles obtained by triangulation from mean separations (Baur, 1971) *are not* in general considered proper measures of mean angles.

The correlations presented in our Figures 6*a* and 6*b* are somewhat improved (see Table 3) when the data from $Yb_2Si_2O_7$, $Er_2Si_2O_7$, and

Table 3

Intercepts, a_o, slopes, b_1, and correlation coefficients, r, for linear regression equations fitted to data in Table 2 and Figs. 5-7. $|t|$s calc. for $H_o:\beta_1 = 0$; all $|t|$'s exceed a two-sided 90% level test

	a_o	b_1	r	$\|t\|$	sample size
Group A of Table 2					
Si-O(br) bond length vs. Si-O-Si angle for silica polymorph data (Fig. 5a)	1.677	-0.0004(2)[1]	-0.48	1.8	12
Si-O(br) bond length vs. -1/cos(Si-O-Si) for silica polymorph data (Fig. 5b)	1.539	0.06(2)	0.57	2.3	12
Si-O bond lengths vs. $\langle O\text{-}Si\text{-}O\rangle_3$ for silica polymorph data (Fig. 5c)	4.094	-0.023(6)	-0.72	3.3	12
Si-O bond length vs. Si-O(est) for silica polymorph data (Fig. 5d)	-0.168	1.1(3)	0.76	3.7	12
Groups A and B[2] of Table 2					
Si-O(br) bond length vs. Si-O-Si angle; Fig. 6a	{1.745	-0.0009(2)	-0.72	4.8	24}
	1.683	-0.0004(2)	-0.45	2.5	27}
Si-O(br) bond length vs. -1/cos(Si-O-Si); Fig. 6b	{1.516	0.08(1)	0.75	5.3	24}
	1.545	0.06(2)	0.58	3.6	27}
Groups A, B, and C[2] of Table 2					
Si-O(br) bond length vs. Si-O-Si angle; Fig. 7a	{1.7008	-0.0005(1)	-0.51	5.1	78}
	1.6841	-0.0004(1)	-0.44	4.3	81}
Si-O(br) bond length vs. -1/cos(Si-O-Si); Fig. 7b	{1.554	0.053(9)	0.53	5.5	78}
	1.561	0.047(9)	0.49	5.0	81}

[1]e.s.d.'s are given in parentheses and refer to the last digit.

[2]The data from thortveitite, $Er_2Si_2O_7$, and $Yb_2Si_2O_7$ were not used to obtain the statistics given in the first row of the data sets enclosed by braces (see text).

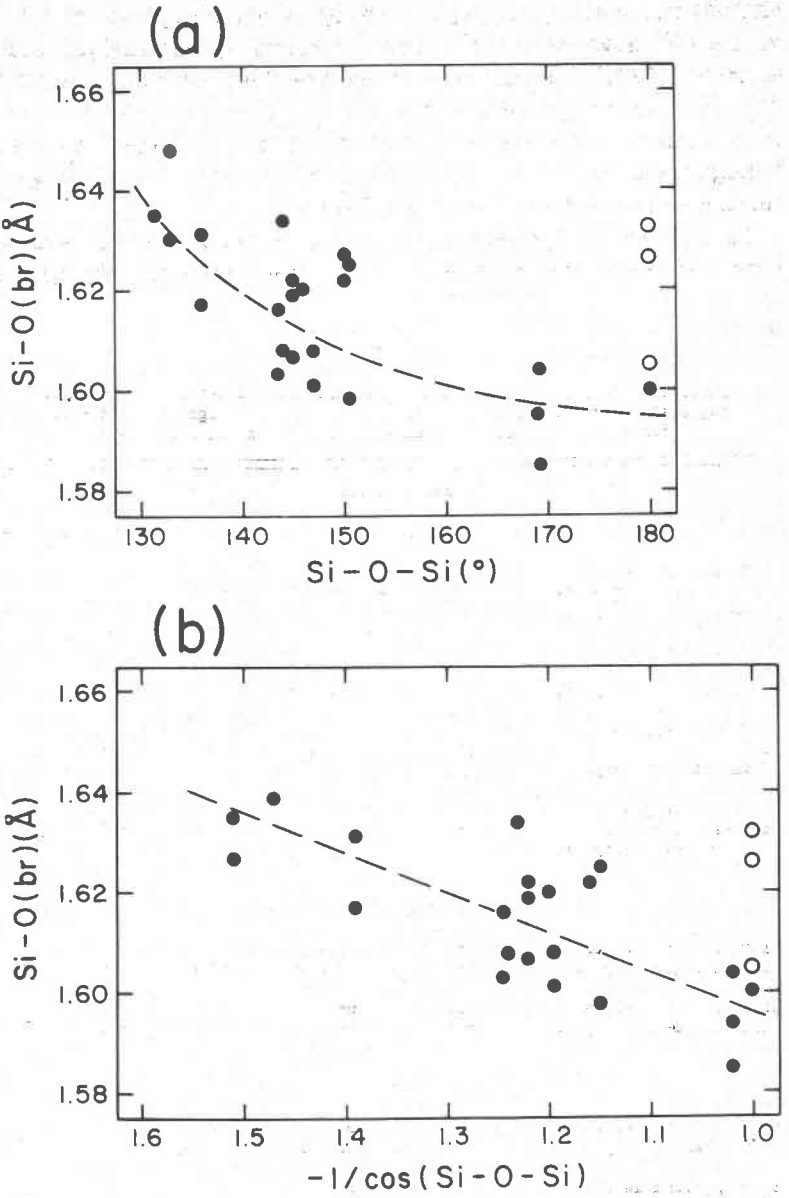

FIG. 6. Scatter diagrams of Si–O(br) bond length data from Table 2, groups A and B, plotted as a function of (*a*) Si–O–Si angle and (*b*) $-1/\cos(\text{Si–O–Si})$. The dashed line in (*b*) is a least squares line. The dashed line in (*a*) is trans-generated from (*b*). The open circle plots are data for thortveitite, $Yb_2Si_2O_7$ and $Er_2Si_2O_7$.

thortveitite are excluded (open symbols in Figs. 6*a* and 6*b*). In these structures ⟨O(br)–Si–O(nbr)⟩$_3$ angles are significantly narrower than ⟨O(nbr)–Si–O(nbr)⟩$_3$ angles, while in the remaining structures ⟨O(br)–Si–O(nbr)⟩$_3$ are either close to or significantly wider than ⟨O(nbr)–Si–O(nbr)⟩$_3$. The n[Si–O(br)] curves in Figure 3 suggest there is no *single* well-defined n[Si–O(br)] versus Si–O–Si relationship, instead a series of curves one for each single value of ⟨O(br)–Si–O(nbr)⟩$_3$. Thus the data for $Yb_2Si_2O_7$, $Er_2Si_2O_7$, and thortveitite belong to a different (though similar) trend compared to the data for the rest of the structures in Table 2 (Group II). A more detailed discussion on the bond length variation in $Yb_2Si_2O_7$, $Er_2Si_2O_7$, thortveitite, and other disilicates will be given elsewhere (Louisnathan and Gibbs, 1972d).

Relative Contributions of $-1/\cos$(Si–O–Si), $\Delta\zeta$(O) and ⟨*CN*⟩ to the Variability of the Si–O(br) Bond Length

As $\Delta\zeta$(O) and the mean coordination number, ⟨*CN*⟩, of oxygen bonded to silicon have also been suggested as determining factors of the Si–O(br) bond length (Baur, 1971), an examination of each in the presence of the others and $-1/\cos$(Si–O–Si) is needed to determine which factors contribute significantly to the regression sum of squares. Therefore, multiple linear and stepwise regression analyses were undertaken for all the data in Table 2 with $-1/\cos$(Si–O–Si), $\Delta\zeta$(O), and ⟨*CN*⟩ as independent variables.

The results are listed in Table 4 in the order ranked by the stepwise

Table 4

Analysis of variance: Multiple linear regression analysis for the data used to prepare Fig. 7 with Si–O(br) bond length as the dependent variable; t(74, 0.90) = 1.7. The order of the independent variable was found by stepwise regression methods.[1]

Independent Variable	|t|	Partial r	Added Regression Sum of Squares	Sample Size
-1/cos(Si-O-Si)	7.0	0.63	0.0043	78
	6.4	0.59	0.0038	81
Δζ(O)	4.2	0.44	0.0020	78
	4.0	0.41	0.0020	81
<CN>	3.2	0.35	0.0005	78
	3.2	0.34	0.0006	81

[1]The data from thortveitite, $Er_2Si_2O_7$, and $Yb_2Si_2O_7$ were not used to obtain the statistics given in the first row of the data sets enclosed by braces (see text).

regression method (*cf.* Draper and Smith, 1966). The $|t|-$ values indicate that all three variables contribute significantly to the variability of the Si–O(br) bond length. In fact, the hypothesis that Si–O(br) bond length might not be dependent on $-1/\cos(\text{Si–O–Si})$ can be rejected at the 0.0005 level. Baur's (1971) implication that the length of Si–O(br) bond depends in part on $\langle CN \rangle$ is borne out by our regression analysis, but the regression coefficient calculated for $\langle CN \rangle$ is significantly smaller [0.0063] than the one [0.0152] used by him to "correct" the observed bond lengths in the four disilicates.

It should be pointed out that the data in Table 2 do not constitute a random sample in the sense that the data are omitted for structures where $\Delta\zeta(\text{O})$ is relatively large and where O(br) is coordinated by more than two atoms. Therefore the regression coefficient calculated for our data probably will not apply to an expanded data set. However, since $\Delta\zeta(\text{O})$ and actual coordination number of O(br) are moderately correlated, we cannot conclude *a priori* whether the magnitude of the slope associated with $\langle CN \rangle$ will be larger or smaller than 0.006 or whether $\langle CN \rangle$ will make a significant contribution to the regression sum of squares in the presence of $\Delta\zeta(\text{O})$.

Plots of Si–O(br) bond length versus Si–O–Si angle for a wide variety of silicates (Cannillo *et al.*, 1968; Brown and Gibbs, 1970) exhibit the same trend as Figures 7*a* or 7*b* (see Table 3) irrespective of the coordination number of the bridging oxygen. Accordingly, it appears that the length of the Si–O(br) bond is related in part to the Si–O–Si angle regardless of the value of $\Delta\zeta(\text{O})$ or $\langle CN \rangle$, with the shorter bonds being involved in the wider angles. Although this result is consistent with a covalent model that includes Si(3*d*) orbital participation, one cannot conclude as indicated earlier that these orbitals are definitely used in the composition of the Si–O bond (Bartell *et al.*, 1970).

The Relationship Between n(Si–O) and the Observed Si–O Bond Length

As both O–Si–O and Si–O–Si angles appear to exert a pronounced role in establishing n(Si–O), we calculated the bond overlap populations for isolated and polymerized tetrahedral ions in ten silicates (Table 5) using the observed O–Si–O and Si–O–Si angles and clamping all Si–O at 1.63Å. The calculation for a valence basis set consisting of silicon 3*s* and 3*p* and oxygen 2*s* and 2*p* atomic orbitals yields bond overlap populations which, when plotted against the observed Si–O distances (Fig. 8), show an apparent linear relation with longer bond lengths being associated with smaller overlap populations. As expected,

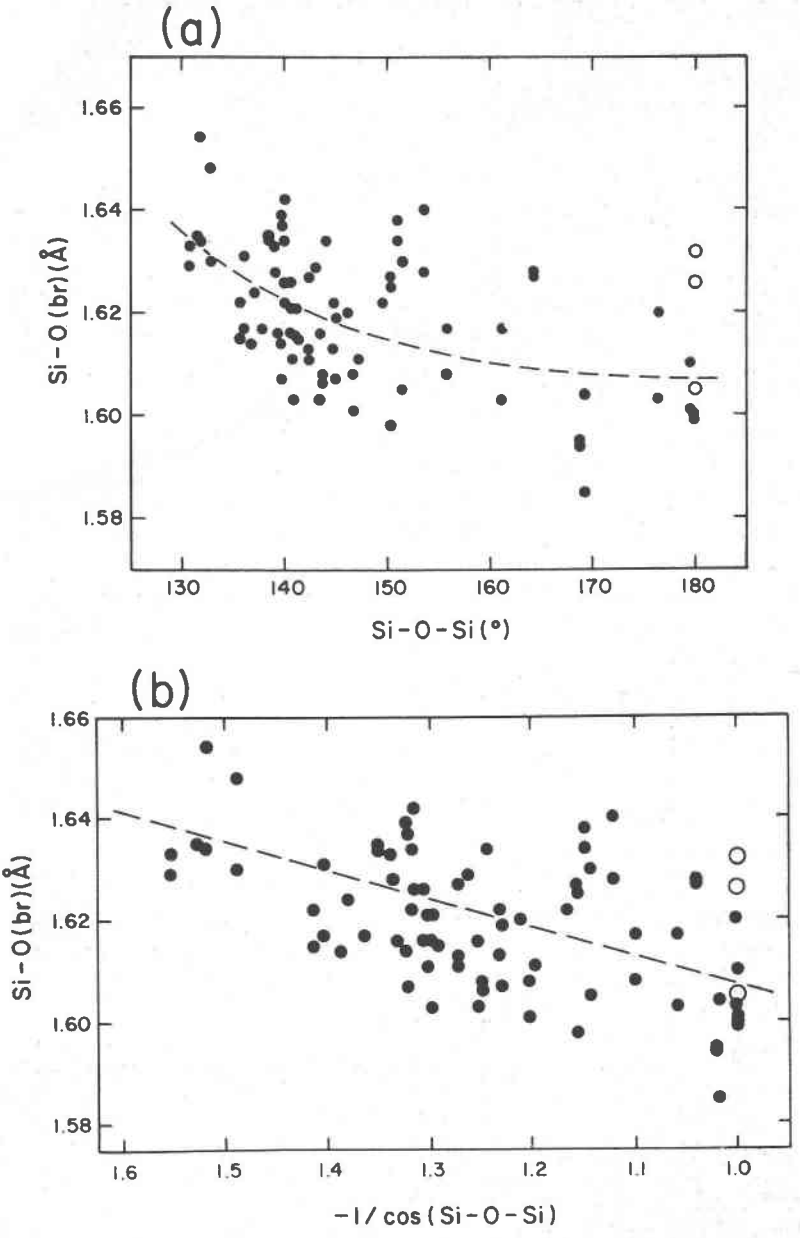

FIG. 7. Scatter diagrams of Si–O(br) bond length data from Table 2, groups A, B and C, plotted as a function of (*a*) Si–O–Si angle and (*b*) $-1/\cos(\text{Si–O–Si})$. The dashed line in (*b*) is a least squares line. The dashed line in (*a*) is transgenerated from (*b*). The open circles are data for thortveitite, $Yb_2Si_2O_7$ and $Er_2Si_2O_7$. The reported e.s.d.'s of the Si–O bond lengths for the structures given in Table 2 are all less or equal to 0.01Å.

Table 5

Bond Lengths and Bond Overlap Populations for Selected Silicates

Structure	Bond	Si-O(br)	Si-O(nbr)	n(Si-O) sp basis Si-O=1.63	n(Si-O) sp basis Si-O=obs	n(Si-O) spd basis Si-O=1.63	n(Si-O) spd basis Si-O=obs	Reference
Dioptase	Si-O(1)	1.646		0.485	0.475	0.747	0.734	Hamil, Gibbs and Ribbe (1971)
	Si-O(1)'	1.645		0.486	0.478	0.756	0.739	
	Si-O(2)		1.617	0.508	0.516	0.942	0.956	
	Si-O(3)		1.600	0.511	0.530	0.946	0.978	
Hemimorphite	Si-O(1)		1.626		0.500		0.922	McDonald and Cruickshank (1967)
	Si-O(2)		1.631		0.505		0.931	
	Si-O(4)	1.627			0.495		0.758	
Thortveitite	Si-O(1)	1.605		0.494	0.506	0.761	0.775	Prewitt (personal communication)
	Si-O(2)		1.627	0.501	0.501	0.923	0.925	
	Si-O(3)		1.628	0.503	0.502	0.926	0.926	
Tourmaline	Si-O(4)	1.623		0.491	0.492	0.758	0.761	Tippe and Hamilton (1971)
	Si-O(5)	1.628		0.488	0.485	0.753	0.752	
	Si-O(6)		1.616	0.510	0.516	0.947	0.960	
	Si-O(7)		1.607	0.508	0.521	0.944	0.968	
Emerald	Si-O(1)	1.604		0.505	0.511	0.778	0.782	Gibbs, Breck and Meagher (1968)
	Si-O(1)'	1.585		0.508	0.530	0.782	0.815	
	Si-O(2)		1.623	0.503	0.503	0.939	0.942	
Beryl	Si-O(1)	1.594		0.505	0.522	0.777	0.795	Gibbs, Breck and Meagher (1968)
	Si-O(1)'	1.595		0.508	0.518	0.782	0.800	
	Si-O(2)		1.620	0.503	0.504	0.939	0.946	
Quartz	Si-O(1)	1.603		0.506	0.516	0.782	0.787	Zachariasen and Plettinger (1965)
	Si-O(3)	1.616		0.504	0.508	0.762	0.768	
Benitoite	Si-O(1)	1.630		0.499	0.499	0.776	0.782	Fischer (1969)
	Si-O(1)'	1.648		0.486	0.471	0.757	0.735	
	Si-O(2)		1.605	0.507	0.521	0.940	0.964	
Margarosanite	Si(1)-O(1)		1.587	0.508	0.537	0.941	0.989	Freed and Peacor (1969)
	Si(1)-O(2)		1.621	0.509	0.514	0.940	0.948	
	Si(1)-O(3)	1.656		0.484	0.470	0.753	0.742	
	Si(1)-O(4)	1.672		0.488	0.465	0.761	0.730	
	Si(2)-O(4)	1.679		0.475	0.453	0.743	0.711	
	Si(2)-O(5)		1.596	0.521	0.545	0.959	0.999	
	Si(2)-O(6)		1.608	0.506	0.523	0.934	0.960	
	Si(2)-O(7)	1.680		0.477	0.434	0.741	0.714	
	Si(3)-O(7)	1.678		0.483	0.462	0.745	0.725	
	Si(3)-O(8)		1.617	0.512	0.523	0.945	0.960	
	Si(3)-O(9)		1.595	0.507	0.538	0.939	0.987	
	Si(3)-O(3)	1.698		0.483	0.445	0.751	0.693	
High pressure $CaSiO_3$	Si(1)-O(1)		1.607		0.521		0.963	Trojer (1969)
	Si(1)-O(2)		1.603		0.523		0.964	
	Si(1)-O(3)	1.683			0.462		0.703	
	Si(1)-O(9)	1.626			0.488		0.771	
	Si(2)-O(3)	1.701			0.440		0.693	
	Si(2)-O(4)		1.589		0.549		1.001	
	Si(2)-O(5)		1.609		0.522		0.959	
	Si(2)-O(6)	1.652			0.469		0.738	
	Si(3)-O(6)	1.669			0.463		0.724	
	Si(3)-O(7)		1.600		0.525		0.971	
	Si(3)-O(8)		1.558		0.555		1.016	
	Si(3)-O(9)	1.681			0.453		0.701	
Ardennite	Si(2)-O(2)		1.604		0.523		0.960	Donnay and Allman (1968)
	Si(2)-O(3)		1.631		0.499		0.918	
	Si(2)-O(8)	1.649			0.451		0.702	
	Si(3)-O(6)		1.631		0.515		0.951	
	Si(3)-O(8)	1.647			0.468		0.723	
Forsterite	Si-O(1)		1.614	0.516	0.526	0.935	0.952	Brown and Gibbs (1972); Louisnathan and Gibbs (1972a)
	Si-O(2)		1.654	0.480	0.470	0.878	0.862	
	Si-O(3)		1.635	0.489	0.487	0.898	0.890	
Datolite	Si-O(1)		1.570	0.506	0.546	0.918	0.987	Foit, Phillips and Gibbs (in preparation)
	Si-O(2)		1.648	0.493	0.484	0.900	0.885	
	Si-O(3)		1.651	0.492	0.482	0.899	0.881	
	Si-O(4)		1.661	0.487	0.469	0.890	0.861	

the overlap populations obtained using observed tetrahedral angles and bond distances in the calculations show a similar but better developed trend when plotted against the observed bond length (Fig. 9). The slopes, intercepts, correlation coefficients, and $|t|-$ statistics calculated for the data in Figures 8 and 9 are given in Table 6 and show that both trends are highly significant.

The curves of Bartell *et al.* (1970) which relate bond length to bond overlap population are similar to those obtained in Figures 8 and 9

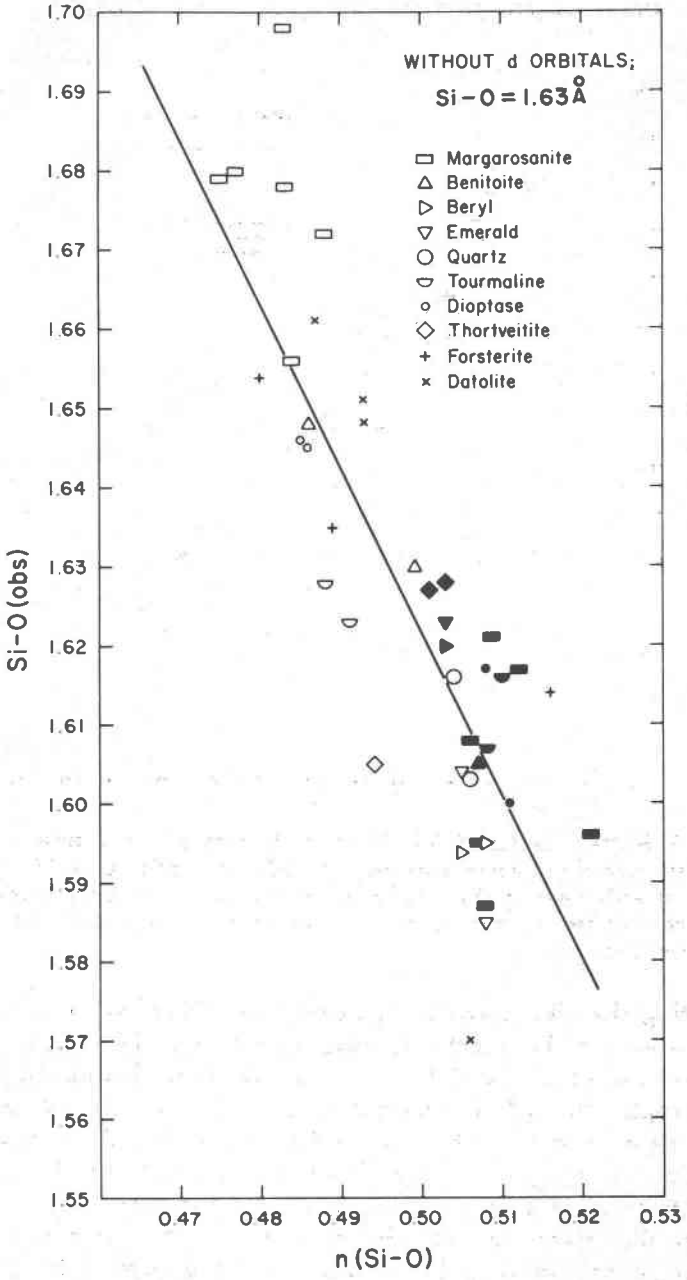

FIG. 8. Scatter diagram of Si–O bond length data plotted against n(Si–O), calculated using observed valence angles, assuming Si–O = 1.63 Å and excluding Si(3d) orbitals for the minerals listed in the upper right. Si–O(br) bonds are indicated by open symbols and Si–O(nbr) bonds by solid ones. Data taken from Table 5.

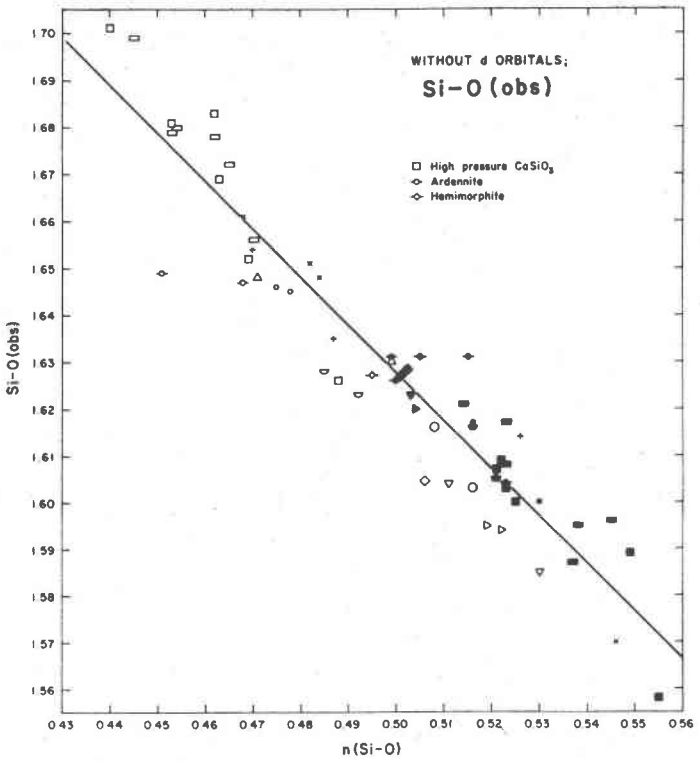

FIG. 9. Scatter diagram of Si–O bond length data plotted against n(Si–O), calculated using the observed distances and angles and excluding Si(3d) orbitals for the minerals listed in the upper right of this figure and Figure 8. Si–O(br) bonds are indicated by open symbols and Si–O(nbr) bonds by solid ones. Data taken from Table 5.

suggesting that the overlap populations calculated for the sulfates, phosphates, and the silicates are comparable when the 3d basis functions are neglected. Correlations can also be made between the Si–O bond length, the net non-bonded geminal populations (*cf.* Bartell *et al.*, 1970), and the net charge differences on Si and O; however, inasmuch as the non-tetrahedral cations were not included in the calculations, such correlations are not appropriate here.

When the valence orbital basis set of silicon is extended to include the five Si(3d) orbitals, the EHMO calculation gives n(Si–O) that again correlate with observed Si–O bond lengths but as two separate trends with the overlap populations for the Si–O(nbr) bonds exceeding those for the Si–O(br) bonds by about 20 percent (Figs. 10 and 11, Table 5). The overlap populations calculated using the observed

tetrahedral angles and all Si–O = 1.63Å are plotted against Si–O(obs) in Figure 10 whereas those calculated using observed distances and angles are plotted against Si–O(obs) in Figure 11. The trends in both scatter diagrams are highly significant as evinced by the $|t|$ —values (Table 6). The correlations are much better developed in Figure 11 where n(Si–O) were calculated using the observed Si–O distances and angles. In addition, the slopes calculated for the Si–O(br) bond trends (Figs. 10 and 11) are steeper than those of the Si–O(nbr) bonds. The Si–O(br) bond trends for the data given in Figures 8 and 9 also appear to be steeper, indicating that the Si–O(br) and Si–O(nbr) bond overlap populations characteristically constitute two distinct populations even when a Si(*sp*) valence basis set is used (Table 4). The difference calculated in n(Si–O) for the Si–O(br) and Si–O(nbr) bonds is due in

Table 6

Intercepts, a_o, slopes, b_1, and correlation coefficients, r, for linear regression equations fitted to data in Figs. 8-11; $|t|$ for $H_o:\beta_1 = 0$

	a_o	b_1	r	$\|t\|$
Observed Si-O bond length vs. n(Si-O) calc. for Si-O = 1.63Å; Fig. 8	2.763	-2.281	-0.84	9.1
Observed Si-O bond length vs. n[Si-O(br)] calc. for Si-O = 1.63; Fig. 8	3.025	-2.822	-0.89	8.3
Observed Si-O bond length vs. n[Si-O(nbr)] calc. for Si-O = 1.63; Fig. 8	2.513	-1.778	-0.77	5.3
Observed Si-O bond length vs. n(Si-O) calc. for obs. Si-O; Fig. 10	2.139	-1.024	-0.94	20.0
Observed Si-O bond length vs. n[Si-O(br)] calc. for Si-O = 1.63; Fig. 8	3.220	-2.076	-0.77	6.0
Observed Si-O bond length vs. n[Si-O(nbr)] calc. for Si-O = 1.63; Fig. 8	2.372	-0.816	-0.70	5.6
Observed Si-O bond length vs. n[Si-O(br)] calc. for obs. Si-O; Fig. 11	2.319	-0.906	-0.94	13.4
Observed Si-O bond length vs. n[Si-O(nbr)] calc. for obs. Si-O; Fig. 11	2.134	-0.548	-0.94	10.2

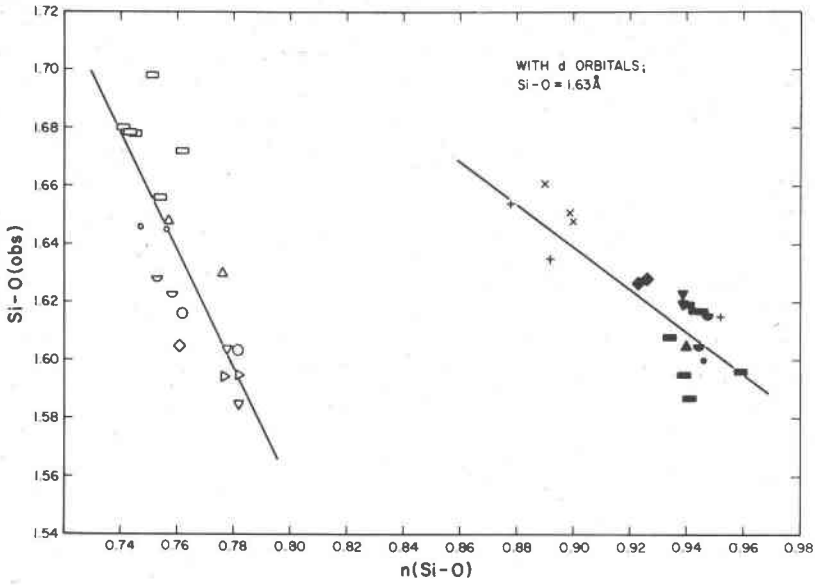

FIG. 10. Scatter diagram of Si–O bond length data plotted against n(Si–O), calculated using observed valence angles, assuming Si–O = 1.63Å and including Si(3d) orbitals for minerals listed in upper right of Figure 8. Data taken from Table 5.

part to the very different environments imposed on these bonds by our modeling of the tetrahedral ion in each silicate as an isolated molecule. According to Bartell *et al.* (1970), part of the difference may also be steric and part may be due to electrostatic forces not reflected in the bond overlap populations.

The n(Si–O) values used to prepare Figures 8 and 10 were calculated with the Si–O distances clamped at 1.63Å but with observed O–Si–O and Si–O–Si angles. Clamping all Si–O distances at 1.63Å may eliminate the bias inherent in using the observed positional parameters, but it can introduce bias because the bond lengths are not allowed to respond to differences in the bond overlap populations estimated by Hückel theory. Moreover, for many complex polymerized SiO_4 ions, the Si–O bond lengths cannot always be clamped at 1.63Å and still retain the observed angles and the continuity of the polymerized unit at the same time. In these cases, it may be possible to obtain a reasonable estimate of the n(Si–O) by using the observed distances and angles in the calculations. This is because well-developed correlations exist between n(Si–O) calculated for Si–O = 1.63Å and those calcu-

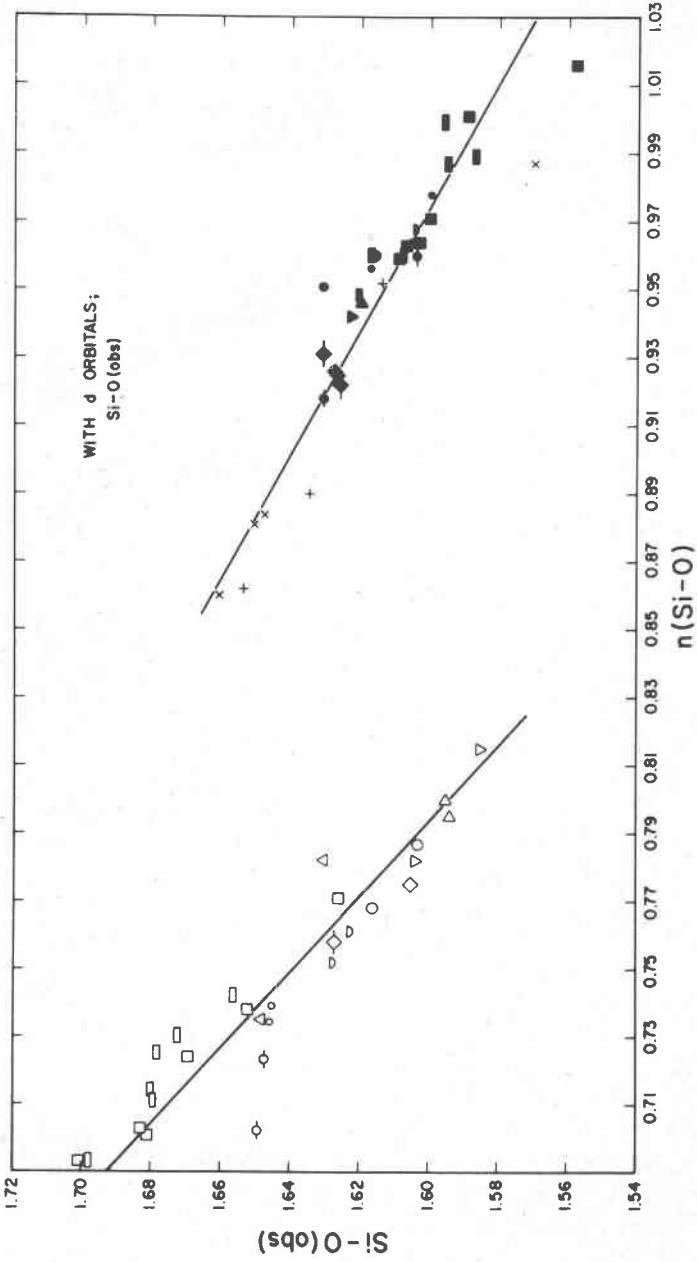

FIG. 11. Scatter diagram of Si–O bond length data plotted against n(Si–O), calculated from observed angles and distances and including Si(3d) orbitals for minerals listed in upper right of Figures 8 and 10. Data taken from Table 5.

lated using the observed positional parameters (Fig. 12) (see Cameron, 1971).

Conclusions

Allen (1970) has implied that EHMO results may be useful in determining a relationship between bond overlap population and bond length relations like that obtained for the hydrocarbons (*cf.* Schug, 1972) but this is the *most* he believes that it can do. Our calculations appear to have been successful in demonstrating such a relationship and suggest that at least part of the Si–O bond length variations observed in the silicates can be rationalized in terms of a covalent bonding model. Our results also imply that the steric details of a silicate cannot be used to *prove* the participation of the Si(3*d*) orbitals in a Si–O bond formation because similar structural trends are predicted when they are omitted and a valence basis set is used. Nevertheless, a covalent bonding model including d–orbital participation permits an understanding of the X–ray emission (Dodd and Glen, 1969; O'Nions and Smith, 1971; Collins *et al.*, 1972) and fluorescence spectra (Urch, 1969, 1971; Collins *et al.*, 1972) and the bond polarizabilities (Revesz, 1971). In addition, it gives a reasonably good account of the trends in Si–O bond length variations. Consequently a covalent bonding model that includes Si(3*d*) orbital involvement should not be dismissed as chemically insignificant. Since EHMO theory fails to take explicit account of electrostatic effects, the senior author and his students are presently undertaking MO calculations at the next level of sophistication which involve the inclusion of the two electron integrals and refinement of the linear coefficients to self consistency as embodied in the CNDO/2 approximation of Pople, Santry, and Segal (1965). These calculations do take ordinary Coulomb interactions into account. It will be of interest, therefore, to compare the CNDO/2 results with those obtained in the present study as well as with those obtained by the *ab initio* method.

Finally, the ultimate goal of any bonding theory for the silicates is to provide some insight into the physical laws that govern atom arrangements, physical properties and stabilities. Molecular orbital theory in its simplest form has been used with moderate success by the organic chemist to rationalize reaction mechanisms, spectra, bond length variations, and shapes for a large number of organic molecules (Streitwieser, 1961). The trends obtained in our study suggest that extended Hückel molecular orbital theory, unlike the extended electrostatic valence rule, may be used to classify and order the bond length variations in the tetrahedral portion of a silicate when $\Delta\zeta(O)$

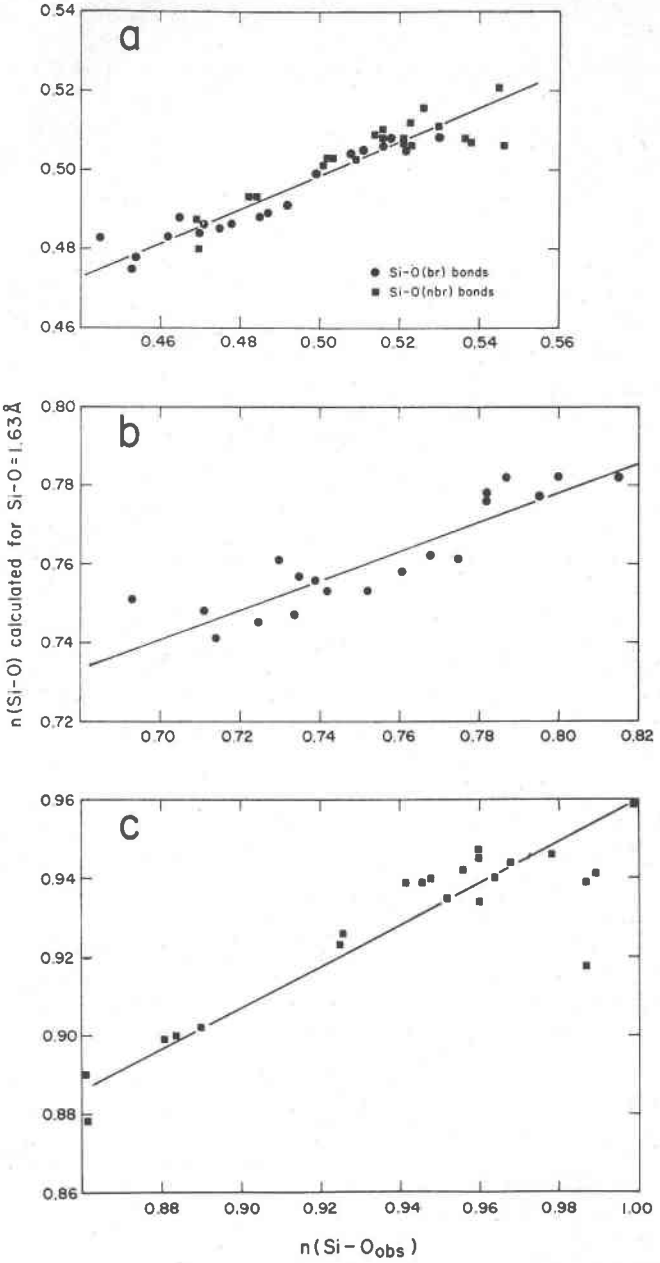

FIG. 12. Bond overlap populations, n(Si–O), calculated with Si–O = 1.63 Å *vs.* n(Si–O) calculated with observed distances, both with observed valence angles.

(a) For Si–O(br) and Si–O(nbr) bonds without Si(3d) orbitals; correlation coefficient $r = 0.94$ (Data from Figs. 8 and 10).

(b) For Si–O(br) bonds with Si(3d) orbitals; $r = 0.90$ (Data from Figs. 9 and 11).

(c) For Si–O(nbr) bonds with Si(3d) orbitals; $r = 0.90$ (Data from Figs. 9 and 11).

$\simeq 0$. Moreover, similar calculations by Urch (1971) have provided valuable insight into the $L_{2,3}$ X-ray fluorescence spectra recorded for silica glass. As the rewards are great, earth scientists are urged to consider the use of MO theory in their interpretation of spectra, physical properties, order–disorder mechanisms, and phase transformations of minerals. Even if application of the theory proves only moderately successful, it should, for example, improve our ability to evaluate evidence bearing on the physical conditions that prevailed when a mineral or a mineral assemblage formed.

Acknowledgments

We are grateful to Drs. G. E. Brown, Jr., R. G. Burns, J. R. Tossell, and D. R. Waldbaum for reviewing the manuscript and making a number of helpful suggestions. Professors F. D. Bloss, D. W. J. Cruickshank, P. H. Ribbe, and J. C. Schug, and Dr. M. W. Phillips are thanked for very helpful discussions and for critically reading the manuscript. G.V.G. gratefully acknowledges the National Science Foundation for its generous support in the form of grants GU-3192, GA-12702, and GA-30864X, and Virginia Polytechnic Institute and State University for providing funds to defray the relatively large computer costs incurred in the study. M.M.H. and S.J.L. gratefully acknowledge the NSF departmental grant (GU-3192) support in the form of research associateships.

Appendix

Stepwise regression analysis is a systematic and objective procedure for recognizing those variables that contribute most significantly to the variation in the response, regardless of their actual entry points into the model. As a first step, a correlation matrix is computed and the variable most highly correlated with the response variable is used to compute a linear regression. The second variable to be entered into the regression is the one whose partial correlation with the response is the largest, *i.e.*, the one that makes the greatest reduction in the error sum of squares. Next, the method examines the contribution the first variable would have made if the second one had been entered first and the first variable second. If the partial F of the first variable is statistically significant at some preselected confidence level, the first variable is retained; otherwise it is rejected. Assuming that both the first and second variables make a significant contribution, the method selects the next variable to be entered, *i.e.*, the one that now has the largest partial correlation with the response given that the first and second variables are in the regression. A regression equation is calculated with all three variables and the third variable is tested for significance. Moreover, partial F tests are again made for the first and second variables to learn whether they should be retained in the regression model. If their partial Fs exceed the preselected level, they are retained; otherwise they are rejected. The procedure is continued and the next most highly correlated variable is entered into the regression. Significance tests are made as before and the method continued with each variable incorporated into the model in a previous step being tested. The method is terminated when all the variables have been considered and no more are rejected (*cf.* Draper and Smith (1966), p. 178–195 for numerical example).

References

Allen, L. C. (1970) Why three-dimensional Hückel theory works and where it breaks down, *In* O. Sinanoğlu and K. B. Wiberg, eds., *Sigma Molecular Orbital Theory*. Yale Univ. Press, New Haven, Connecticut, 227–248.

——— (1972) The shape of molecules. *Theoret. Chim. Acta* **24**, 117–131.

Almenningen, A., O. Bastianse, V. Ewing, K. Hedberg, and M. Traetteberg (1963) The molecular structure of disiloxane, $(SiH_3)_2O$. *Acta Chem. Scand.* **17**, 2455–2460.

Anderson, J. S., and J. S. Ogden (1969) Matrix isolation studies of Group-IV oxides. I. Infrared spectra and structures of SiO, Si_2O_2, and Si_3O_3. *J. Chem. Phys.* **51**, 4189–4196.

Araki, T., and T. Zoltai (1969) Refinement of a coesite structure. *Z. Kristallogr.* **129**, 381–387.

Bartell, L. S., L. S. Su, and H. Yow (1970) Lengths of phosphorus-oxygen and sulfur-oxygen bonds. An extended Hückel molecular orbital examination of Cruickshank's d_π–p_π picture. *Inorg. Chem.* **9**, 1903–1912.

Basch, H., A. Viste, and H. B. Gray (1965) Valence orbital ionization potentials from atomic spectra data. *Theoret. Chim. Acta* **3**, 458–464.

Baur, Werner (1970) Bond length variation and distorted coordination polyhedra in inorganic crystals. *Trans. Amer. Crystallogr. Ass.* **6**, 125–155.

——— (1971) The prediction of bond length variations in silicon-oxygen bonds. *Amer. Mineral.* **56**, 1573–1599.

Bent, H. A. (1968) Tangent-sphere models of molecules: VI. Ion-packing models of covalent compounds. *J. Chem. Ed.* **45**, 768–778.

Boer, F. P., and W. N. Lipscomb (1969) Molecular SCF calculations for SiH_4 and H_2S. *J. Chem. Phys.* **50**, 989–992.

Bokii, N. G., and Y. T. Struchkov (1968) Structural chemistry of organic compounds of the nontransition elements of Group IV (Si, Ge, Sn, Pb). *Zh. Strukt.: Khim.* **9**, 633–672 [transl. *J. Struct. Chem.* **9**, 633–672].

Boyd, D. R., and W. N. Lipscomb (1969) Electronic structures for energy-rich phosphates. *J. Theoret. Biol.* **25**, 403–420.

Brown, B. E., and S. W. Bailey (1964) The structure of maximum microcline. *Acta Crystallogr.* **17**, 1391–1400.

Brown, G. E., and G. V. Gibbs (1969) Oxygen coordination and the Si–O bond. *Amer. Mineral.* **54**, 1528–1539.

———, and ——— (1970) Stereochemistry and ordering in the tetrahedral portion of silicates. *Amer. Mineral.* **55**, 1587–1607.

———, ———, and P. H. Ribbe (1969) The nature and variation in length of the Si–O and Al–O bonds in framework silicates. *Amer. Mineral.* **54**, 1044–1061.

Busing, W. R., and H. A. Levy (1964) The effect of thermal motion on the estimation of bond lengths diffraction measurements. *Acta Crystallogr.* **17**, 142–146.

Cameron, M. (1971) *The Crystal Chemistry of Tremolite and Richterite: A Study of Selected Anion and Cation Substitution.* Ph.D. thesis, Virginia Polytechnic Institute and State University, Blacksburg, Virginia.

Cannillo, E., G. Rossi, and L. Ungaretti (1968) The crystal structure of macdonaldite. *Accad. Naz. Lincei* **45**, 399–414.

Clementi, E., and D. L. Raimondi (1963) Atomic screening constants from SCF functions. *J. Chem. Phys.* **38**, 2686–2689.

CODA, A., A. DAL NEGRO, AND G. ROSSI (1967) The crystal structure of krauskopfite. *Accad. Naz. Dei Lincei* **42**, 859–873.

COLLINS, G. A. D., D. W. J. CRUICKSHANK, AND A. BREEZE (1972) *Ab initio* calculations on the silicate ion, orthosilicic acid and their $L_{2,3}$ X-ray spectra. *J. Chem. Soc., Faraday Trans. II,* **68**, 1189–1195.

COTTON, A. F., AND G. WILKINSON (1969) *Advanced Inorganic Chemistry.* John Wiley and Sons, New York, N. Y.

COULSON, C. A. (1939) The electronic structure of some polyenes and aromatic molecules. VII. Bonds of fractional order by the molecular orbital method. *Proc. Royal Soc., Ser. A,* **169**, 413–428.

CRUICKSHANK, D. W. J. (1961) The role of 3*d*-orbitals in π-bonds between (a) silicon, phosphorus, sulfur, or chlorine and (b) oxygen or nitrogen. *J. Chem. Soc.* **1077**, 5486–5504.

DALLINGA, G., AND P. ROSS (1968) Semi-empirical prediction of bond lengths and conformations. *Rec. Trav. Chim.* **87**, 906–915.

DODD, C. G., AND G. L. GLEN (1969) A survey of chemical bonding in silicate minerals by X-ray emission spectroscopy. *Amer. Mineral.* **54**, 1299–1311.

DOLLASE, W. A. (1965) Reinvestigation of the structure of low cristobalite. *Z. Kristallogr.* **121**, 369–377.

——— (1968) Refinement and comparison of the structures of zoisite and clinozoisite. *Amer. Mineral.* **53**, 1882–1898.

——— (1969) Crystal structure and cation ordering of piedmontite. *Amer. Mineral.* **54**, 710–717.

——— (1971) Refinement of the crystal structures of epidote, allanite and hancockite. *Amer. Mineral.* **56**, 447–464.

DONNAY, G., AND R. ALLMAN (1968) Si_3O_{10} groups in the crystal structure of ardennite. *Acta Crystallogr.* **B24**, 845–855.

DRAPER, N. R., AND H. SMITH (1966) *Applied Regression Analysis.* John Wiley and Sons, Inc., New York.

FINGER, L. W. (1969) The crystal structure of grunerite. *Mineral. Soc. Amer. Spec. Pap.* **2**, 95–100.

——— (1970) Refinement of the crystal structure of anthophyllite. *Carnegie Inst. Washington Year Book,* **68**, 283–288.

FISCHER, K. (1969) Verfeinerung der Kristallstruktur von Benitoit $BaTi[Si_3O_9]$. *Z. Kristallogr.* **129**, 369–377.

FREED, R. L., AND D. R. PEACOR (1969) Determination and refinement of the crystal structure of margarosanite, $PbCa_2Si_3O_9$. *Z. Kristallogr.* **128**, 213–228.

FYFE, W. S. (1954) The problem of bond type. *Amer. Mineral.* **39**, 991–1004.

GAVIN, R. M., JR. (1969) Simplified molecular orbital approach to inorganic stereochemistry. *J. Chem. Ed.* **46**, 413–422.

GIBBS, G. V. (1966) The polymorphism of cordierite. I. The crystal structure of low cordierite. *Amer. Mineral.* **51**, 1068–1087.

——— (1969) Crystal structure of protoamphibole. *Mineral. Soc. Amer. Spec. Pap.* **2**, 101–109.

———, D. W. BRECK, AND E. P. MEAGHER (1968) Structural refinement of hydrous and anhydrous synthetic beryl, $Al_2(Be_3Si_6)O_{18}$ and emerald, $Al_{1.9}Cr_{0.1}(Be_3Si_6)O_{18}$. *Lithos,* **1**, 275–285.

GILLESPIE, R. J. (1960) Bond angles and the spatial correlation of electrons. *J. Amer. Chem. Soc.* **82**, 5978–5983.

GRIFFITH, W. P. (1969) Raman studies on rock-forming minerals. Part 1. Orthosilicates and cyclosilicates. *J. Chem. Soc.* **(A)**, 1372–1377.

HAMIL, M. M., G. V. GIBBS, AND P. H. RIBBE (1971) The location of the hydrogen atoms in the water molecule of dioptase. [abstr.]. *Geol. Soc. Amer. Abstr. Programs,* **3**, 315.

———, G. V. GIBBS, L. S. BARTELL, AND H. YOW (1971) A comparison of Si–O bond lengths with EHMO bond overlap populations. [abstr.]. *Geol. Soc. Amer. Abstr. Programs,* **3**, 589.

HOFFMANN, R. (1963) An extended Hückel theory. I. Hydrocarbons. *J. Chem. Phys.* **39**, 1397–1412.

LAUGHON, R. B. (1971) The crystal structure of kinoite. *Amer. Mineral.* **56**, 193–200.

LAZAREV, A. N. (1964) Polymorphism of molecules and complex ions in oxygen compounds of silicon and phosphorus. Report 1. Nature of the Si–O–Si bonds and values of the valence angles of oxygen. *Izv. Akad. Nauk SSSR, Ser. Khim.* **2**, 235–241.

LIEBAU, F. (1961) Untersuchungen über die Grösse des Si–O–Si Valenz–winkels. *Acta Crystallogr.* **14**, 1103–1109.

LOUISNATHAN, S. J., AND G. V. GIBBS (1971) A comparison of Si–O distances in the olivines with the bond overlap populations predicted by the extended Hückel molecular orbital (EHMO) theory. [abstr.]. *Geol. Soc. Amer. Abstr. Programs,* **3**, 636.

———, AND ——— (1972a) The effect of tetrahedral angles on Si–O bond overlap populations for isolated tetrahedra. *Amer. Mineral.* **57**, 1614–1642.

———, AND ——— (1972b) Variation of Si–O distances in olivines, soda melilite and sodium metasilicate as predicted by semiempirical molecular orbital calculations. *Amer. Mineral.* **57**, 1643–1663.

———, AND ——— (1972c) Aluminum–Silicon distribution in zunyite. *Amer. Mineral.* **57**, 1068–1087.

——— AND ——— (1972d) The Si–O bond length variation in pyrosilicates. [abstr.] *Geol. Soc. Amer. Abstr. Programs,* **4**, 580–581.

———, AND J. V. SMITH (1971) Crystal structure of tilleyite: Refinement and coordination. *Z. Kristallogr.* **132**, 288–306.

MCDONALD, W. S., AND D. W. J. CRUICKSHANK (1967a) A reinvestigation of the structure of sodium metasilicate, Na_2SiO_3. *Acta Crystallogr.* **22**, 37–43.

——— AND ——— (1967b) Refinement of the structure of hemimorphite. *Z. Kristallogr.* **124**, 180–191.

Meagher, E. P. (1967) *Polymorphism of Cordierite.* Ph.D. thesis, Penn. State University, University Park, Pennsylvania.

MITCHELL, J. T., F. D. BLOSS, AND G. V. GIBBS (1971) Examination of the actinolite structure and four other *C2/m* amphiboles in terms of double bonding. *Z. Kristallogr.* **133**, 273–300.

MITCHELL, K. A. R. (1969) The use of outer *d* orbitals in bonding. *Chem. Rev.* **69**, 157–178.

MULLIKEN, R. S. (1955) Electronic population analysis on LCAO–MO molecular wave functions. I. *J. Chem. Phys.* **23**, 1833–1846.

NOLL, W. (1956) Characteristika der Siloxan–bindung in polymeren Anionen (Silikaten) und polymeren molekülen (Siliconen). *Fortschr. Mineral.* **34**, 63–84.

——— (1968) *Chemistry and Technology of Silicones, 2nd ed.* Academic Press, Inc., New York, N.Y.

OBERHAMMER, H. (1972) The molecular structures of cyclosiloxanes. [abstr.] *Fourth Austin Symposium on Gas Phase Molecular Structure,* 11–12.

O'Nions, R. K., and D. G. W. Smith (1971) Bonding in SiO_2 and Fe_2O_3 by oxygen $K\alpha$ X-ray emission spectra. *Nature,* **231**, 130–133.

Papike, J. J., and J. R. Clark (1968) The crystal structure and cation distribution of glaucophane. *Amer. Mineral.* **53**, 1156–1173.

———, M. Ross, and J. R. Clark (1969) Crystal chemical characterization of clinoamphiboles based on five new structure refinements. *Mineral. Soc. Amer. Spec. Pap.* **2**, 177–186.

Pauling, Linus (1929) The principles determining the structure of complex ionic crystals. *J. Amer. Chem. Soc.* **51**, 1010–1026.

——— (1939) *The Nature of the Chemical Bond, 1st ed.* Cornell Univ. Press, Ithaca, N. Y.

——— (1952) Interatomic distances and bond character in the oxygen acids and related substances. *J. Phys. Chem.* **56**, 361–365.

——— (1960) *The Nature of the Chemical Bond, 3rd ed.* Cornell Univ. Press, Ithaca, N. Y.

Phillips, M. W., P. H. Ribbe, and G. V. Gibbs (1971) Refinement of the crystal structure of danburite. [abstr.] *Geol. Soc. Amer. Abstr. Programs* **3**, 338.

Pople, J. A., D. P. Santry, and G. A. Segal (1965) Approximate self-consistent molecular orbital theory. I. Invariant procedures. *J. Chem. Phys.* **43**, 129–135.

Revesz, A. G. (1971) π-bonding and delocalization effects in SiO_2 polymorphs. *Phys. Rev. Lett.* **27**, 1578–1581.

Ribbe, P. H., H. D. Megaw, and W. H. Taylor (1969) The albite structures. *Acta Crystallogr.* **25**, 1503–1518.

Richards, W. G., and J. A. Horsley (1970) Ab initio *Molecular Orbital Calculations for Chemists.* Clarendon Press, Oxford.

Robinson, P. D., and J. H. Fang (1970) The crystal structure of epididymite. *Amer. Mineral.* **55**, 1541–1549.

Schug, J. C. (1972) *Introductory Quantum Chemistry.* Holt, Rinehart and Winston, Inc., New York, N. Y.

Shannon, J., and L. Katz (1970) The structure of barium silicon niobium oxide, $Ba_3Si_4Nb_6O_{20}$: A compound with linear silicon–oxygen–silicon groups. *Acta Crystallogr.* **B26**, 105–109.

Shannon, R. D., and C. T. Prewitt (1969) Effective ionic radii in oxides and fluorides. *Acta Crystallogr.* **B25**, 925–946.

Smolin, Y. I., and Y. F. Shepelev (1970) The crystal structure of the rare earth pyrosilicates. *Acta Crystallogr.* **B26**, 484–492.

Stewart, D. B., and P. H. Ribbe (1969) Structural explanation for variations in cell parameters of alkali feldspar with Al/Si ordering. *Amer. J. Sci., Schairer Vol.* **267–A**, 444–462.

Streitwieser, A. (1961) *Molecular Orbital Theory for Organic Chemists.* John Wiley and Sons, Inc., New York, N.Y.

Tippe, A., and W. C. Hamilton (1971) A neutron diffraction study of the ferric tourmaline, buergerite. *Amer. Mineral.* **56**, 101–113.

Trojer, F. J. (1969) The crystal structural of a high-pressure polymorph of $CaSiO_3$. *Z. Kristallogr.* **130**, 185–206.

Urch, D. S. (1969) Direct evidence for $3d$–$2p$ π-bonding in oxy-anions. *J. Chem. Soc.* **A**, 3026–3028.

——— (1971) X-ray emission spectroscopy. *Quart. Rev.* **25**, 343–364.

Urusov, V. S. (1967) Chemical bonding in silica and silicates. *Geokhimiya,* **4**, 399–412 [Eng. trans. *Geochem. Int.* **4**, 350–362 (1967)].

VERHOOGEN, J. (1958) Physical properties and bond type in Mg–Al oxides and silicates. *Amer. Mineral.* **43**, 552–579.

WIEDNER, D. J., AND G. SIMMONS (1972) Elastic properties of alpha quartz and the alkali halides based on an interatomic force model. *J. Geophys. Res.* **77**, 826–856.

WOLFSBERG, M., AND L. HELMHOLZ (1952) The spectra and electronic structure of the tetrahedral ions MnO_4^-, CrO_4^{--} and ClO_4^-. *J. Chem. Phys.* **20**, 837–843.

ZACHARIASEN, W. H., AND H. A. PLETTINGER (1965) Extinction in quartz. *Acta Crystallogr.* **18**, 710–714.

Manuscript received, January 14, 1972; accepted for publication, June 6, 1972.

Note added in proof by GVG: The electrostatic valence rule proposed by Pauling (1929) and extended by Baur (1970) was originally conceived to characterize strengths of ionic-type bonds and local charge balance in stable ionic crystals. It is evident, however, that the model seems to apply equally well to compounds in which the bonds have a relatively large amount of covalent character. For these compounds, Pauling (1960, 547–548, Footnote 64) has indicated that "if the bonds resonate among the alternative positions, the valence of the metal atom will tend to be divided equally among the bonds to the coordinated atoms, and a rule equivalent to the electrostatic valence rule would express the satisfaction of the valences of the nonmetal atoms." Pauling's statement implies [1] that the strength of an electrostatic bond, s, can be equated with bond number, n (Pauling, 1947, *J. Amer. Chem. Soc.* **69**, 542–553); [2] that the correlations between ζ(O) and the length of the Si–O bond (Smith, 1953, *Amer. Mineral.* **38**, 643–661; Baur, 1970) are similar to the well known bond-length bond-number curve for carbon-carbon bonds; and [3] that the charges on bonded atoms are small in agreement with his electroneutrality principle (Pauling, 1956, *General Chemistry,* W. H. Freeman and Co., 236–237). The inference that n and s are equivalent is consistent with the observation that ζ(O) and n(Si–O) are inversely correlated (Louisnathan and Gibbs, 1972b). Although Baur calls his model the extended electrostatic valence rule, he is careful to note that the correlation between observed Si–O bond length and ζ(O) could be interpreted in terms of Cruickshank's (1961) double bonding model as well as the Born model for ionic crystals.